ARR No. 3J13

NATIONAL ADVISORY COMMITTEE FOR AERONAUTICS

WARTIME REPORT

ORIGINALLY ISSUED
October 1943 as
Advance [redacted] Report 3J13

WIND-TUNNEL INVESTIGATION OF WING DUCTS ON A SINGLE-ENGINE PURSUIT AIRPLANE

By W. J. Nelson and K. R. Czarnecki

Langley Memorial Aeronautical Laboratory
Langley Field, Va.

NACA

WASHINGTON

NATIONAL ADVISORY COMMITTEE FOB AERONAUTICS

ADVANCE [redacted] REPORT

L-407

WIND-TUNNEL INVESTIGATION OF WING DUCTS OB A SINGLE-ENGINE PURSUIT AIRPLANE

By W. J. Nelson and K. R. Czarnecki

SUMMARY

A study of several ducts installed in the wings of a model of a conventional single-engine pursuit airplane has been made in the NACA full-scale tunnel to determine the influence of inlet design and cooling-air flow on the pressure losses within the duct and on the aerodynamic characteristics of the airplane. The effect of propeller operation on the total-pressure losses in the ducts symmetrically located behind the upgoing and downgoing blades is shown by tests of two of the inlets.

Large differences in total pressure at the radiator occurred as a result of variations in (1) the inlet-velocity ratio, (2) the lift coefficient, (3) the shape and position of the inlet, (4) the slope of tho diffuser axis, and (5) propeller operation. A compromise fixed inlet, which had high pressure recovery over a satisfactory range of flight attitudes, low drag, and a high maximum lift coefficieat, was designed. Rotation inside the slipstream of the propeller effected appreciable differences in the pressure losses in similar ducts symmetrically Located behind the upgoing and downgoing propeller blades.

INTRODUCTION

An investigation of ducts installed in the wings and fuselage of a modal of a conventional single-engine pursuit-type airplane has been made in the NACA full-scale tunnel. The results of the tests of ducts with inlets located on top of the fuselage close to the propeller and on the bottom of the fuselage behind the leading edge of the wing are presented in references 1 and 2. The present report contains the results of tests of ducts located within the wings of the model.

Previous investigations of wing ducts at Langley Memorial Aeronautical Laboratory have, in general, been confined to tests of isolated wings, and the effects of fuselage interference and propeller slipstream have not been extensively studied (references 3 to 5). These effects have been included in the present investigation by testing a complete airplane model with propeller removed and with propeller operating. The effects on the duct characteristics and airplane performance of variations in the geometry of the ducts and in the air flow through the ducts have also been investigated. Total- and static-pressure measurements and force tests were made over a range of angle of attack and inlet-velocity ratio with various ducts installed in one or both wings of the model. The ducts tested differed widely in size and position of the inlet opening, in inlet-lip contour, in inclination of the inlet plane and diffuser axis to the wing chord, and in outlet position.

SYMBOLS

C_L lift coefficient

ΔC_D increment of drag coefficient due to duct

C_{D_d} calculated increment of drag due to losses in inlet and diffuser

ΔC_{D_i} calculated increment of drag coefficient due to losses in duct and radiator

ΔC_{D_e} increment of drag coefficient due to external drag of duct $(\Delta C_D - \Delta C_{D_i})$

T_c propeller thrust coefficient $\left(\frac{\text{thrust}}{\rho V_o^2 D^2}\right)$

q dynamic pressure

E total pressure (referenced to free-stream static pressure)

p static pressure (referenced to free-stream static pressure)

Δp pressure drop across orifice plate

Q quantity rate of low

Q/V_0 air-flow parameter

V_1/V_0 inlet-velocity ratio

η duct efficiency $\left(\frac{Q\,\Delta p}{\Delta C_D\, V_0}\right)$

ρ air density

D propeller diameter

S wing area

A_1 inlet area

c_f flap chord

α angle of **attack** of thrust axis relative to free-stream direction

β propeller blade setting at 0.75 radius

Subscripts:

0 in free stream

1 in duct inlet

2 at front fact? of orifice plate

3 in outlet of duct

max maximum

APPARATUS AMI) TESTS

A **photograph** of the model mounted in the NACA full-scale tunnel is shonn as figure 1. The general arrangement and basic dimensions of the model are given in figure 2. The wing area is 170 square feet. The model was equipped with **a** cuffed propeller 10 feet in diameter that was driven by a **25-horsepower** electric motor located in the fuselags.

The wing section at the center line of the duct, the ordinates of **which** are given in table I, is a modification of an NACA 230-series airfoil. Center-line sections through the various ducts and the principal dimensions of

the ducts are given in figure 3 and in tables II and III. These sections were approximately constant between the vertical walls of the ducts at wing stations 21¾ and 47¼ inches from the fuselage center line. The transition from the vertical side walls in the duct to the rounded ends at the inlet was accomplished in the forward part of the diffuser. The inboard side of each inlet, except inlet 7, was 2¼ inches from the fuselage; the span of inlet 7 was reduced to 22 inches and the distance between the end of the inlet and the fuselage was increased to 4 inches. All of the inlets were fixed except inlet 6, which was fitted with a flapped lower lip that could be adjusted to provide smooth entry of the air flow into the duct over a wide range of angle of attack. Photographs of typical inlet installations (inlets 2 and 4) are presented as figure 4 and the outlets are shown as figure 5. Each outlet was fitted with an adjustable flap by which the air flow through the system was controlled.

Aluminum orifice plates with *holes* 3/4 inch in diameter were used to simulate radiators. The conductivity of the plates was varied by plugging some of the holes in accordance with the technique of reference 6.

The quantity of air flowing through the various duct systens was determined from measurements of total and static pressures at the duct outlet. Total-pressure measurements in front of the radiator and in the outlet were used in calculating the duct losses.

Pressure measurements were nade with the propeller removed for all the inlets; inlets 4 and 5 were also tested with the propeller operating at thrust coefficients simulating high-speed and climbing flight. The inlets tested with power on were installed symmetrically about the thrust fine to determine the effects of slipstream rotation on the inlet and diffuser losses.

\$he effect of the various duct installations on the drag and on the maximum lift of the model was determined by force tests. The drag coefficient of the model with and without ducts installed was determined from propeller-removed tests at airspeeds of *63* and 102 miles per 'hour. These tests were made over a range of lift coefficient from -0.25 to 0.55. The maximum-lift tests were made at an airspeed of approximately 53 miles per hour with the landing flaps deflected 45° and retracted.

RESULTS AND DISCUSSION

The results of the tests have Seen analyzed with consideration for the following requirements for satisfactory duct operation: (1) high pressure recoveries at the face of the heat exchanger for a range of flight attitudes from high speed to climb, (2) low drag of the duct installation, and (3) satisfactory maximum-lift characteristics of the ducted. wing sections. The results are presented in seetions in which the following are discussed: pressure losses in the inlet and diffuser, pressure drop through the radiator, static pressure at the duct outlet, and effects of variations i.n the geometry of the inlets and air flow into the ducts on the drag and on the maximum lift of the complete model.

Pressure Losses ahead of Radiator

The pressure Losses in diffusers of the types investigated in the present tests have beer: shown to be small when the boundzry-layer thickness at the duct inlet is small and when the diffuser is alined with the approaching flow. If the inlet lips are not properly alined vith the approaching flow, disturbances of the air flow will occur at the inlet and the losses in the diffuser will increase. Large changes in the pressures ahead of the radiator are shown in figures 6 to 13 to have resulted from varying (1) the inlet-velocity ratio, (2) the lift coefficient of the wing section at the duct inlet, and (3) the shape and position of the inlet lips.

Effect of inlet-velocity ratio.- Previous investigations of duct openings at the leading edge of a wing or fuselage have shomn that the flon at the inlet becomes unstable at inlet-velocity ratios below approximately 0.35. In this range of low inlet-velocity ratios, the pressure losses within the duct may be excessiva and the local velocity over the lips of the inlet will be high. As the value of inlet-velocity ratio is increased above this range, the stability of the air entering the duct will increase and. the local velocity over the lips of the inlet will decrease. Most of the present tests have therefore been restricted to a r nge of inlet-velocity ratios above 0.4.

The average total pressure at the face of a radiator behind inlet 4 is shown in figure 6 as a function of the inlet-velocity ratio at lift coefficients of 0.12, 0.47, and 0.89. At $C_L = 0.12$, the inlet and the diffuser losses were essentially constant over the range of V_1/V_0 from 0.6 to 1.4, At $C_L = 0.47$ and 0.89, the losses increased rapidly mitb V_1/V_0. Tne individual pressures recorded for the different lift coefficients at 18 paints on the front of the radiator are presented in figure 7 to facilitate analysis of the losses. These data show high recovery and uniform distribution of total pressure over a wide range of V_1/V_0 at $C_L = 0.12$ and over a very small range of V_1/V_0 at $C_L = 0.47$ and 0.89.

The change in alinement affected by varying the inlet-velocity ratio at a lift coefficient of about 0.5 is shown diagrammatically in the accompanying sketches. In the

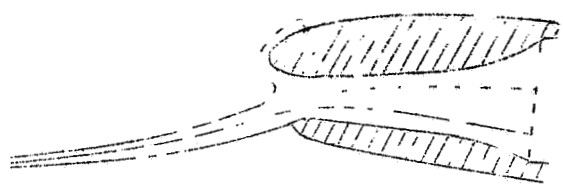

(a) $V_1/V_0 < 0.35$

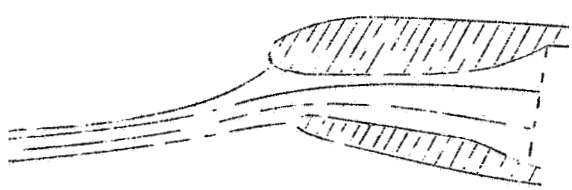

(b) $V_1/V_0 \approx 0.5$

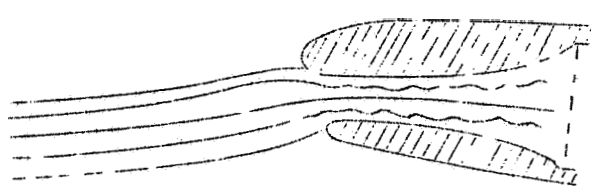

(c) $V_1/V_0 > 1.0$

unstable range of inlet-velocity ratios, that is, at $V_1/V_0 < 0.35$, the air flow breaks down at the inlet and the air tends to flow intermittently through the duct and over the upper lip of the inlet (sketch (a)). At $V_1/V_0 \approx 0.5$, the expansion ahead of the inlet is uniform and the air enters the duct smoothly, as shown in sketch (b). At higher inlet-velocity ratios there is a substantial increase in the local velocities over the lips of the inlet at a point just inside the duct. This increase in local velocity at $V_1/V_0 > 1.0$ causes separation from the lips of the inlet as shown in sketch (c).

The data presented in figure 7 and in several of the following figures show a considerable decrease in total pressure over the inboard end of the radiator. This effect is a result of the proximity of the inlets to the fuselage. Part of the fuselage boundary layer, upon reaching the stagnation point at the leading edge of the wing, moves outward to the lower pressure region at the inlet and is carried into the duct.

Effect of lift coefficient.- The average total pressure at the face of the radiator is shown as a function of lift coefficient in figure 8, in which data from figure 6 have been cross-plotted at several values of inlet-velocity ratio. High recoveries with inlet 4 were obtained over the widest range of lift coefficient at inlet-velocity ratios between 0.4 and 0.6. At values of the lift coefficient higher than that of best recovery the losses increased rapidly. The pressure distributions of figure 7 indicate that decreases in recovery which result from increases in lift coefficient were caused by separation from the lower wall of the duct.

The flow at the inlet and through the diffuser is shown schematically at two lift coefficients in the accompanying sketches (d) and (e). At low values of the lift coefficient (sketch (d)), both lips of the inlet were alined with the flow at the leading edge of the wing;

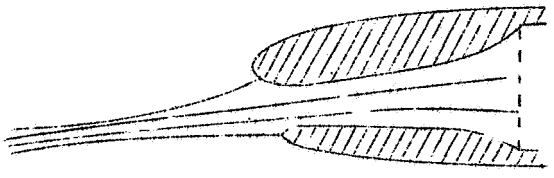

(d) Low lift coefficient

a

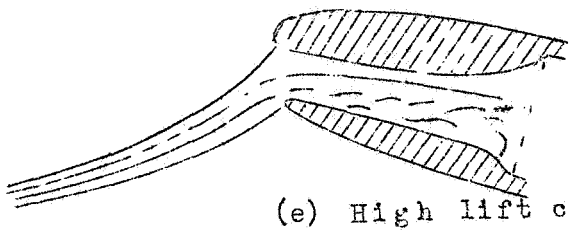

(e) High lift coefficient

hence there was no disturbance of the flow into the diffuser and the pressures at the radiator were uniform and high. Increases in lift coefficient are accompanied by a downward movement of the stagnation points on both lips of the inlet, by an increase in static pressure on the lower surface of each lip, and by a decrease in static pressure over the upper surface of the lips. At high lift coefficients, therefore, air enters the upper part of the duct smoothly but. separates from the lower wall of the duct, as shown in sketch (e).

Effect of inlet design and diffuser inclination. - A summary of the data taken in tests of inlets 1, 2, 4, and 5 (fig. 9) shows that the position of the inlet lips and the inclination of the diffuser have a marked effect upon the average total pressure at the radiator. Unfortunately, it was not feasible to maintain constant inlet-velocity ratio throughout these tests; the effect of changes in Inlet-velocity ratio are therefore included in the results.

The individual measurements from which the averages in figure 9 were obtained are presented in figure 10. Behind inlet 1, mhich has the entrance plane nearly perpendicular to the wing chord and to the diffuser axis? the total pressure at the radiator mas $0.95q_0$ at $C_L = 0.12$; the losses increased rapidly with lift coefficient, however, until at $C_L = 0.89$ only $0.22q_0$ vas recovered at the front of the radiator. A slight extension of the upper lip that turned the plane of the inlet downward 6° (inlet 2) increased the average pressure recovery $0.03q_0$ at $C_L = 0.12$ and $0.29q_0$ at $C_L = 0.89$. The influence of slight differences in the diffusers behind inlets 1 and 2 is considered negligible, Further extension of the upper lip (inlet 4) was beneficial at higher values of C_L but detrimental at $C_L = 0.12$.

The slope of the fnlet plane of inlet 5 was similar to that of inlet 4; however the diffuses was inclined downward 11° instead of 4.58. This increase in slope of the diffuser axis decreased the pressure recovery at $C_L = 0.12$ from $0.95q_0$ to $0.86q_0$; but, at $C_L > 0.33$, higher pressures were measured behind inlet 5. The differences in recovery increased rapidly with lift coefficient and reached $0.20q_0$ at $C_L = 0.89$.

The effect of inclinations of inlet plane and diffuser axis is shown diagrammatically in sketches (f) to (k). At low lift coefficients, tho flow into the duct is smooth when the inlet plane is approximately perpendfeular to the chord line and the diffuser axis is alined with the flow at the leading edge of the wing (sketch (f)). Inclining the plane of the inlet or the diffuser axis downward results in a tendency of the flow to separate just inside the upper lip (sketches (g) and (h)). At high lift coefficients, separation of the air flow from the lower lip will occur if the plane of the inlet or tbe diffuser axis is riot alined mith the approaching air stream (sketches (i) and (j)). The flow into an inlet having both the diffuser axis and the plane of the iniet alined with the flow at a high lift coefficient is shown in sketch (k).

Decreasing the conductivity *of* the radiator had little effect upon the pressure losses through the inlet and diffusers, as may be noted by comparing the results in figures 10 and 11.

Inlet 6 was fitted with a flap by which the effective slope of the inlet face and the area of the opening could be increased. The effect of inlet-flap position on the average total pressur at the faze of the radiator is shown as a function of lift coefficient in figure 12. These results shorn that opening the flap at $C_L = 0.12$ decreased the average total pressure 15 percent; at $C_L > 0.12$, however, substantial gains were effected by opening the flap. At these higher values of C_L, there was some separation over the nose of the vane, as shown by the reduced pressures near the top of the radiator (fig. 13). The average pressure recovery with this arrangement mas lower than that obtained behind the Getter fixed inlets; however, it is likely that this design could be improved with further study.

Effect of propeller operation.- If the cooling air passes through the propeller disk before entering the duct,

Low lift coefficient

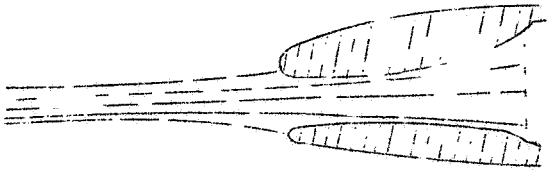

(f)

Inlet plane perpendicular to and diffuser axis parallel to wing chord

High lift coefficient

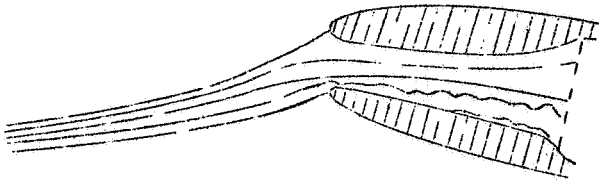

(i)

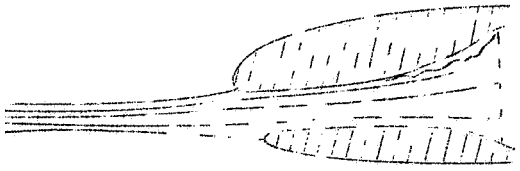

(g)

Inlet plane inclined downward and diffuser axis parallel to wing chord

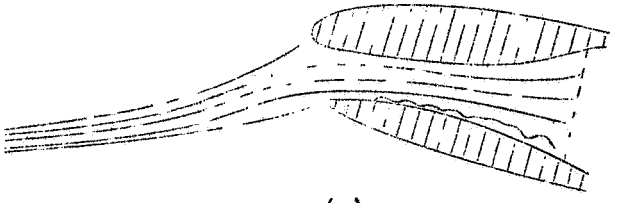

(j)

(h)

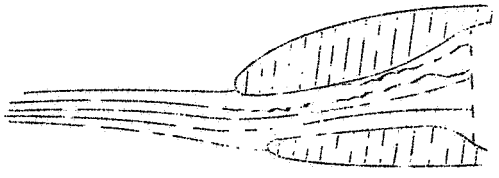

(k)

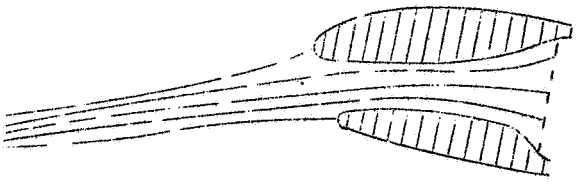

Inlet plane and diffuser axis inclined downward from wing chord

it approaches the inlet vith a total pressure greater than tnat of the free stream and with an angular velocity. If the effect of unequal pressure distribation behind an inclined propeller is assumed to be small, the greatest part of nny difference in the pressure measured in similar ducts symmetrically located in the right and left wings mill occur as a result or" the difference in the angle at which the air stream approaches the inlets. With right-hand propeller rotation, the effective angles of attack of the inboard sections of the left wing will increase; whereas the effective angles of attack of the right wing will decrease. The slipstream rotation will therefore change the alinement with the approaching air stream of the inlet lips on both wings.

The effects of the misalinement due to propeller operation on the total pressure recovery at the radiator, with inlet 4 installed on the model, are shonn in figures 14 and 15. In the nigh-speed sttitade ($C_L = 0.12$, $\beta = 60^\circ$, and $T_c = 0.02$), the total pressures on the side of the upgoing propeller blades were 13 to 24 percent higher than those measured behind the downgoing blades. (See fig. 14.) Under conditions simulating full-power climb ($C_L = 0.47$, $\beta = 40^\circ$, and $T_c = 0.11$), the difference between the recover; in the right *a?* left ducts increased considerably, as shown by compariso of figures 14 and 15.

Similar inlets, conforming to the profile designated inlet 5, mere tested in both wings with the propeller operating and with tne propeller removed. Data obtained in the power-on tests are presented in figures i6 to 19. In the tests with the propeller removed (fig. 9(a)), the pressure recovery behind this inlet reached *a* maximum of $0.97q_0$ at $C_L = 0.47$; therefore, it was to be expected that, at $C_L = 3.12$, pressure losses with power on would be higher behind the downgoing blades because ths effective C_L would be loner on this wing. The increased losses in the right duct more than offset the increase in total pressure due to the propeller slipstream; thus, with power on, the total pressure ahead of the radiator was equal to or slightly leas than that, recorded with the propeller removed. On the side of the upgoing blades, the increase in local lift coefficient reduced the duct losses and thus caused a substantial increase in available total pressure. In the climbing attitude, the total pressure at the right radiator was 15 to 30 percent greater than at *the* left radiator. (See figs. 18 and 13.)

Static Pressure at Duct Exit

The design of a complete duct system requires a knowledge not only of the pressure losses in the duct but also of the static pressure at the duct outlet. Data taken in these tests show the influence of lift; coefficient, outlet-flap deflection, and inlet design on the static pressure at the duct exits located in tne lower surface and at the trailing edge of tho wing.

The static pressure at an outlet in the lower surface of the wing is shown in figure 2C as a fanction of lift coefficient and outlet-flap position. Inlet 4 vas installed for these tests. At low lift coefficients, the static pressure in this oatlet, with exit flaps closed, exceeded free-stream static pressure by $C.30q_0$; the difference between the static pressure at tne outlet and free-stream static pressure increased with lift coefficient and reached $0.38q_0$ at $C_L = 0.89$. Deflecting the outlet flap 45° reduced the static pressure within the outlet $0.55q_0$.

Measurements of static pressure in the trailing-edge outlet with inlet 4 installed aye presented in figure 21. The reduction in static pressure obtained by deflecting the upper flap at the trailing-edge outlet (fig. *3)* was considerably larger at low than at high lift coefficients. The change in static ressure obtained by deflecting the landing flap (fig. 21) was greatest when 'she upper flap mas neutral; however, the lowest **pressure** was obtained with both flaps deflected.

Changes in the duct system ahead of the radiator, with the outlet located in the Lower surface of the wing, are shown in figure 22 to have effected appreciable variations in the static pressure at the outlet. These variations occur as a result of unequal losses of total pressure and of differences in air flow **through** the various ducts.

The influence of the propeller slipstream on the static **pressure** at outlets symmetrically located in the lower surface of both wings is shonn in table IV. Because rotation in the slipstream increases the lift coefficient on the left wing and decreases it on the right, the static pressure with the propeller operating was expected to be higher at the outlet in the left wing and lower at the outlet in the **right** wing. In the high-speed attitude, the change in the outlet static pressure effected by the slipstream **was** very small and reached a maximum value of $0.06q_0$. Under conditions simulating full-paver climb, with outlet flaps full open,

the static pressure decreased $0.30q_0$ to $0.44q_0$ in the outlet of the right duct and $0.13q_0$ to $0.17q_0$ in the left outlet from the value measured with the propeller removed.

Although comparative tests of the various outlets were not made with the landing flaps deflected, a qualitative analysis of the effect of deflecting the landing flaps is possible. Inasmuch as the air flow through a duct is a function of the static pressure at the outlet and the static pressure over the lower surfece of the wing increases with flap deflection, the flow through the duct with the bottom outlet would decrease with flap deflection. With the top or trailing-edge outlets, deflection of the landing flaps should increase the flow thnough the duct.

Drag

The results of the drag tests gre summarized in table V. The increase in drag coefficient resulting from various duct installations is considered in two parts: (1) the increment associated with the passage of cooling air through the ducts, internal drag, and. (2) the increment resulting from disturbances of the external flow. The internal drag is equal to the momentum lost by the cooling air in passing through the ducts and radiator; and, by neglecting compressibility and heat effects, the drag coefficient ΔC_{D_i} may be calculated from the equation

$$\Delta C_{D_i} = \frac{2Q}{SV_0}\left(1 - \sqrt{\frac{H_3}{H_0}}\right)$$

Division of this increment into diffuser drag and radiator drag has been accomplished by substituting the pressure at the radiator for H_3 in the foregoing equation and subtracting the resulting increment from ΔC_{D_i}. The inlet and diffuser drag calculated from this substitution is slightly in error because some of the retarded air from the fuselage boundary layer has entered the duct,

The external drag is the difference between the total-drag increment of the duct installation, which is determined from force tests, and the internal drag. These componet-drag ccefficients and other pertinent data taken with the model in the high-speed attitude ($C_L = 0.12$) are

summarized in table V. Analysis of the results shows that, for the same cooling-air flow, the total-drag increment was slightly lower for tile small sharp-lip inlets 1 and 6, The diffuser drag is dependent on the total-pressure losses within the diffuser; thase losses have been discussed in a previous section. The radiator drag is a function of radiator resistance, velocity through the core, and distribution of the flow through the unit.

The duct efficiency, defined as the ratio of useful work to total work is given in the last column of table V to facilitate comparison of the various ducts. It is observed that inlets 1 and. 6 gave higher efficiency at $C_L = 0.12$ and $V_1/V_0 = 0.6$ than any of the other ducts. At lift coefficients corresponding to climbing flight, however, the pressure losses behivd these inlets were excessive.

Maximum Lift Coefficient

The results of several tests to determine the influence of the various wing-duct instnllations on the maximum lift coefficient of the model are presented in figures 23 to 27. A summary of these results is presented in table VI.

The maximum lift coefficient of the model in the basic condition - without wing ducts, with the propeller removed, and with the landing flaps neutral - vas 1.35. Installation of ducts with inlet 2 and with the outlets located on the lower surface of both wings reduced $C_{L_{max}}$ to 1.07. With the duct outlet located on the upper surface of the wing, $C_{L_{max}}$ was 1.16. The smaller reduction in $C_{L_{max}}$ obtained by moving the outlet to the upper surface of the wing is largely a result of an increase in V_1/V_0 and of improved flow at the duct inlet.

Several modifications of the upper lip of inlet 2 were tested to determine the effects of the position and the leading-edge radius of the upper lip of the inlet on the maximum lift coefficient of the model. These tests were made mith the duct outlet in the lower surface of the wing. The upper lip of the inlet was extended $1\frac{1}{8}$ inches to form the profile designated inlet 3. A coinparison of the curves of figure 24 shows that this change resulted in an increase of 0.16 in $C_{L_{max}}$. Inlet 4 differed from inlet 3 in the lending-edge radius of the upper lip and in the height of

the inlet opening (fig. 3); $C_{L_{max}}$ was 0.12 higher for this inlet than for inlet 3. It should be noted that $C_{L_{max}}$ with inlet 4 installed was the same as $C_{L_{max}}$ measured with the smooth wing.

Inlet 4 mas also tested with the duct outlet located at the trailing edge of the wing. For this condition of the model, the value of $C_{L_{max}}$ mas 0.09 lower than for the reference condition (fig. 26).

With the diffuser inclined downward 11° (inlet 5), $C_{L_{max}}$ exceeded by 0.07 that measured- on the basic model. Similar increases in $C_{L_{max}}$ due to ring ducts were reported in a previous investigation {reference 3). The upper lip of inlet 7 was the same as that of inlet 5; the lower lip, however, was cut back to increase tne slope of the inlet plane. With this duct installed in only the left wing, $C_{L_{max}}$ was 0.01 higher than that obtained with the smooth wing.

The effects of propeller operation on the maximum lift coefficient of the model with inlet 5 installed in both wings are shown in figure 27. At $T_c = 0.02$, $C_{L_{max}}$ was increased 0.03 with flaps retracted and 0.12 with flaps deflected 45° above the value of $C_{L_{max}}$ neasured with the propeller removed.

SUMMARY OF RESULTS

The results of the present study of several ducts installed in the wings of a model of a conventional single-engine pursuit airplane mounted in the NACA full-scale tunnel are summarized as follows:

1. The pressure recovery ahead of a radiator installed in a wing duct was determined principally by (1) the inlet-velocity ratio, (2) the lift coefficient, and (3) the shape and location of the inlet lips and diffuser.

2. Highest pressure recoveries at the front face of the radiator were obtained at inlet-velocity ratios from 0.4 to 0.6.

3. A duct with the plane of the inlet opening perpendicular to the wing chord and with a diffuser parallel to

the chord line gave highest pressure recoveries at low lift coefficients. At high lift coefficients, best pressure recovery was obtained when the upper lip was extended ahead of the lower lip and the diffuser was inclined downward.

4. Because of rotation in the slipstream of a single propeller, the pressure recovery in a duct located behind the upgoing blades was not the same as that in a similar duct symmetrically located behind the downgoing blades. Best design practice would require different ducts on the right and the left wings of the airplane.

5. The total pressure over the inboard end of the radiator was low if the end of the inlet was close to the fuselage.

6. The use of outlet flaps reduced the static pressure in the exit as much as 60 percert of the free-stream dynamic pressure.

7. An inlet with well-cambered upper lip properly alined with the flow at the leading edge of the wing effected. a small increase in the maximum lift coefficient of the airplane; whereas substantial decreases in the maximum lift coefficient were effected by ducts with the inlet plane perpendicular to the chord line and by inlet lips with small leading-edge radii.

8. The best compromise fixed inlet tested in the present investigation had an upper lip with a large leading-edge radius conforming approximately to the contour of the original wing, a lower lip cut back to turn the inlet plane downward 70° to the chord line, and a diffuser inclined approximately 10° to the wing chord.

9. Aa inlet with an adjustable lower lip appeared feasible in cases in which fixed inlets were unsatisfactory because of an extreme range of inlet-velocity ratio and lift coefficient.

Langley Memorial Aeronautical Laboratory,
Bational Advisory Committee for Aeronautics,
Langley Field, Va.

REFERENCES

1. Nelson, W. J., and Czarnecki, K. R.: Wind-Tunnel Investigation of Carburetor-Air Inlets. NACA A.R.B., Fsb. 1942.

2. Czarnecki, K. R., and Nelson, W. J.: Wind-Tunnel Investigation of Hear Underslung Fuselage Ducts. NACA A.R.R. No. 3I21, Sept. 1943.

3. Silverstein, Abe, and Nickle, F. R.: Preliminary Full-Scale Wind-Tunnel Investigation of Wing Ducts for Radiators. NACA A.C.R., March 1938.

4. Nickle, F. R., and Freeman, Arthur B.: pull-Scale Wind-Tunnel Investigation of Wing Cooling Ducts. NACA A.C.R., Oct. 1938.

5. Harris, Thomas A., and Recant, Isidore G.: Investigation in the 7- by 10-Foot Wind Tunnel of Ducts for Cooling Radiators within an Airplane Wing. Rep. No. 743, NACA, 1942.

6. Czarnecki, K. R.: Pressure-Drop Characteristics of Orifice Plates Used to Simulate Radiators. BACA A.R.R., March 1942.

TABLE I

AIRFOIL ORDIMATES
[Percent wing chord]

	Upper	Lower
	0	
1.0		
	3.8	
5.0	5.4	-2.7
10.0	7.3	-4.0
15.0	8.3	-4.7
20.0	8.8	-5.3
25.0	9.0	-5.6
30.0	8.9	-5.8
40.0	8.5	-5.7
50.0	7.6	-5.3

TABLE III

OUTLET ORDINATES
[Percent wing chord)

x	Bottom		Top		T.E.	
	y_b	y_c	y_b	y_c	y_b	y_c
40	6.9	-4.3	-3.8	7.1	7.1	-4.1
45	3.2	-5.1	-.2	7.6	6.0	-3.6
50	-.8	-5.1	3.4	7.4	5.0	-3.1
55	-3.3	----	5.2	---	4.2	-2.7
60	-4.2	----	5.8	---	3.7	-2.2
65	-4.2	----	5.5	---	3.5	-1.8
70	----	----	4.9	---	3.3	-1.5
80	----	----	----	---	2.9	-1.0
90	----	----	----	---	---	-.5
100	----	----	----	---	---	.0

Flap	c_f
1	20.5
2	7.7
3	11.5
Landing	25.0

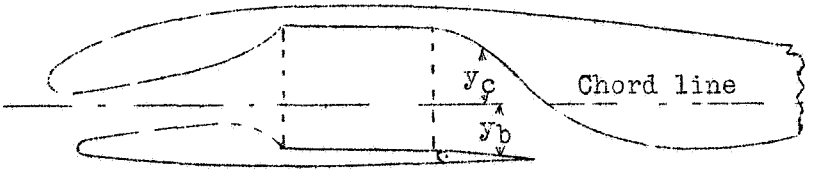

TABLE II

INLET ORDINATES
[Percent wing chord]

Inlet / x	1				2				3				4				5				6				7			
	y_a	y_b	y_c	y_d	y_a	y_b	y_c	y_d	y_a	y_b	c	y_d	y_a	y_b	y_c	y_d	y_a	y_b	y_c	y_d	y_a	y_b	y_c	y_d	y_a	y_b	y_c	y_d
-1.0	---	---	---	---	---	---	---	---	3.6	2.8	---	--	3.8	2.1	---	--	--	---	---	---	---	---	---	---	--	--	---	---
-.5	---	---	---	---	---	---	---	---	4.1	2.7	---	--	4.4	1.9	---	--	--	---	---	---	---	---	---	---	--	--	---	---
0	2.3	2.3	1.9	1.9	---	---	---	---	4.5	2.8	---	--	4.9	1.8	---	--	--	---	---	---	---	---	---	---	--	--	---	---
.5	3.3	1.9	1.5	2.5	4.0	2.9	---	---	4.8	2.8	---	--	5.3	1.9	---	--	--	---	---	---	---	---	---	---	--	--	---	---
1.0	3.7	1.9	1.4	2.7	4.3	2.9	---	---	5.0	2.9	---	--	5.7	2.0	---	--	--	---	---	---	---	---	---	---	--	--	---	---
1.5	4.1	2.0	1.4	2.9	4.7	3.0	2.1	2.8	5.3	3.0			6.0	2.1				---	---	---	---	---	---	---			---	---
2.5	4.7	2.0	1.4	3.2	5.2	3.1	2.0	3.4	5.6	3.1			6.5	2.3				---	---	---	---	---	---	---			---	---
5.0	5.8	2.3	1.4	3.8	6.2	3.4	2.0	4.0	6.3	3.4			7.2	2.8				1.1	---	---	---	2.3	1.1			---	---
7.5	6.6	2.6	1.4	4.3	6.9	3.7	1.9	4.3	6.9	3.7			7.7	3.5				1.4	2.8	4.2		2.4	1.0			---	---
10.0	7.3	3.0	1.4	4.6	7.5	4.0	1.9	4.8					8.0	4.0				1.8	2.5	4.5		2.7	1.0			---	---
12.5	7.9	3.4	1.4	4.9	8.0	4.4	2.0	4.9					8.3	4.4				2.3	2.1	4.8		3.0	1.0			---	---
15.0	8.3	3.8	1.5	5.1	8.3	4.8	2.0	5.1					8.5	4.8				2.8	1.9	5.1		3.3	1.0			2.1	4.4
17.5	8.5	4.4	1.8	5.3	8.6	5.2	2.1	5.3					8.6	5.2				3.3	1.6	5.3		3.8	1.2			1.6	4.7
20.0	8.7	5.0	2.1	5.5	8.8	5.8	2.2	5.4					8.8	5.8				3.9	1.5	5.4		4.1	1.4			1.5	5.0
22.0	---	6.0	2.8	---	---	6.5	2.6	---					---	6.5				4.6	1.7	5.5		4.5	1.8			1.8	5.2
																		6.0	2.5	---		5.8	2.6			6.0	2.5
	x_U = 0.5 y_U = 2.4 R_U = 0.5 x_L = 0.4 y_L = 1.9 R_L = 0.4 A_1 = 0.467				x_U = 0.7 y_U = 3.3 R_U = 0.5 x_L = 1.8 y_L = 2.5 R_L = 0.5 A_1 = 0.690				x_U = -0.6 y_U = 3.3 R_U = 0.6 x_L = 1.8 y_L = 2.5 R_L = 0.5 A_1 = 0.690				x_U = -0.4 y_U = 2.9 R_U = 0.9 x_L = 1.8 y_L = 2.5 R_L = 0.5 A_1 = 0.565				x_U = 2.8 y_U = 2.1 R_U = 1.1 x_L = 4.4 y_L = 3.5 R_L = 0.6 A_1 = 0.544				x_U = 2.1 y_U = 2.6 R_U = 0.4 x_L = 2.7 y_L = 1.4 R_L = 0.4 A_1 = 0.443				x_U = 2.8 y_U = 2.1 R_U = 1.1 x_L = 10.9 y_L = 4.0 R_L = 0.1			

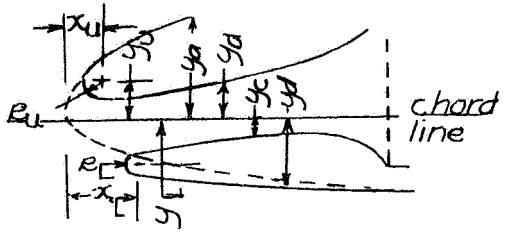

TABLE IV

SUMMARY OF SLIPSTREAM EFFECTS ON

STATIC PRESSURE IN DUCT OUTLET

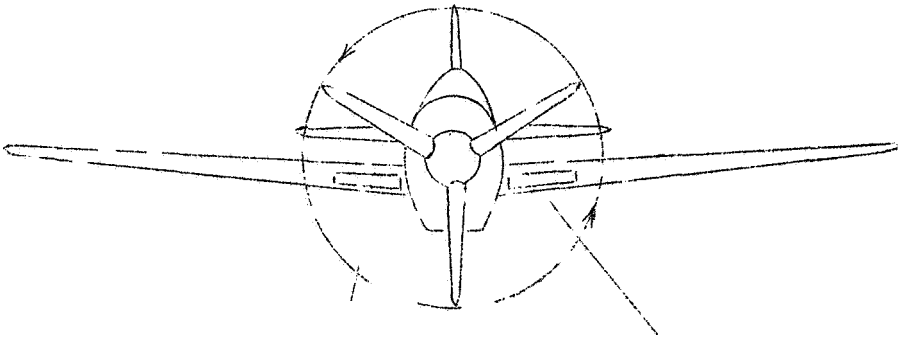

Inlet	C_L	Right wing				Left wing			
		Propeller removed		Propeller operating		Propeller removed		Propeller operating	
		V_1/V_0	p_3/q_0	V_1/V_0	p_3/q_0	V_1/V_0	p_3/q_0	V_1/V_0	p_3/q_0
4	0.12	-----	-----	0.59	0.24	0.52	0.41	0.51	0.40
		-----	-----	.65	.25	.63	.30	.63	.36
	.47	-----	-----	1.37	-.45	1.08	-.16	1.08	-.30
		-----	-----	1.39	-.46	1.19	-.20	1.12	-.33
5	0.12	0.59	0.26	0.57	0.23	0.52	0.32	0.51	0.37
		.62	.28	.66	.26	.61	.28	.62	.32
	.47	.98	-.49	1.78	-.79	1.08	-.50	2.03	-.64
		1.11	-.41	1.79	-.85	1.11	-.48	1.93	-.65

TABLE V

SUMMARY OF RESULTS OF DRAG TESTS OF SEVERAL WING DUCTS

Inlet	Outlet		$\Delta p/q_2$	Q/V_0	V_1/V_0	ΔC_D		C_{D_d}	C_{D_i}	C_{D_e}	η
	Position	Flap	(design)			At 50 mph	At 100 mph				
1	Bottom	3	5.8	0.28	0.59	0.0006	0.0003	0.00005	0.00052	-0.0002	0.9
	Bottom	2	5.8	----	----	------	.0007	-------	-------	-------	---
	Bottom	3	11.0	26	.55	.0008	.0007	.00003	.00061	.0001	.6
2	Bottom	3	5.8	----	----	[1]0.0018	[1]0.0020	-------	-------	-------	---
	Bottom	2	5.8	[1]0.66	0.49	------	[1].0035	[1]0.00038	0.00224	[1]0.0013	0.4
	Bottom	2	11.0	[1].58	42	[1] 0038	[1].0042	[1].00004	[1].00254	[1].0017	.3
4	Bottom	3	5.8	0.35	0.62	------	0.0009	0.00012	0.00067	0.0002	0.6
	Bottom	2	5.8	----	----	0.0010	.0010	-------	-------	------	---
	Bottom	2	5 8	.36	.64	------	[1].0025	.00011	.00085	.0004	.5
	T.E.	1	5.8	[1].64	[1].56	[1].0028	[1].0021	[1].00025	[1].00180	[1].0003	.4
	Bottom	2	11.0	31	.54	.0014	.0012	-------	-------	-------	---
5	Bottom	3	5.8	0.56	0.52	------	[1]0.0022	[1]0.00028	[1]0.00128	[1]0.0009	0.3
	Bottom	2	5.8	[1].69	.64	------	[1].0035	[1].00024	[1] 00148	[1].0020	.3
	Bottom	3	11.0	[1].50	46	------	[1] 0027	[1].00036	[1].00170	[1].0010	.4
	Bottom	2	11.0	[1].59	.55	------	[1].0032	[1].00028	[1].00234	[1] 0009	.4
6	Bottom	3	5.8	0.34	0.76	0.0007	0.0006	0.00008	0.00068	-0.0001	0.9
	Bottom	2	5.8	----	----	------	.0004	-------	-------	-------	---

[1]Air flowing through ducts in both wings.

TABLE VI

SUMMARY OF MAXIMUM-LIFT TESTS

[Propeller removed, landing flaps neutral, outlet flaps closed]

Inlet	Outlet	$C_{L_{max}}$	$\Delta C_{L_{max}}$	Remarks
Sealed	Sealed	1.35	-------	Basic condition, complete model.
Sealed	Sealed	1.30	-------	Basic condition, except tail surfaces removed.
1	Bottom	1.26	-0.09	Duct in only left wing.
2	Bottom	1.07	-.28	Ducts in both wings.
2	Top	1.16	-.19	Do.
3	Bottom	1.23	-.12	Do.
4	Bottom	1.35	.00	Do.
4	T.E.	1.21	-.09	Ducts in both wings, tail surfaces removed.
5	Bottom	1.42	.07	Ducts in both wings.
6	Bottom	1.21	-.14	Duct in only left wing, inlet flap open.
7	Bottom	1.36	.01	Duct in only left wing.

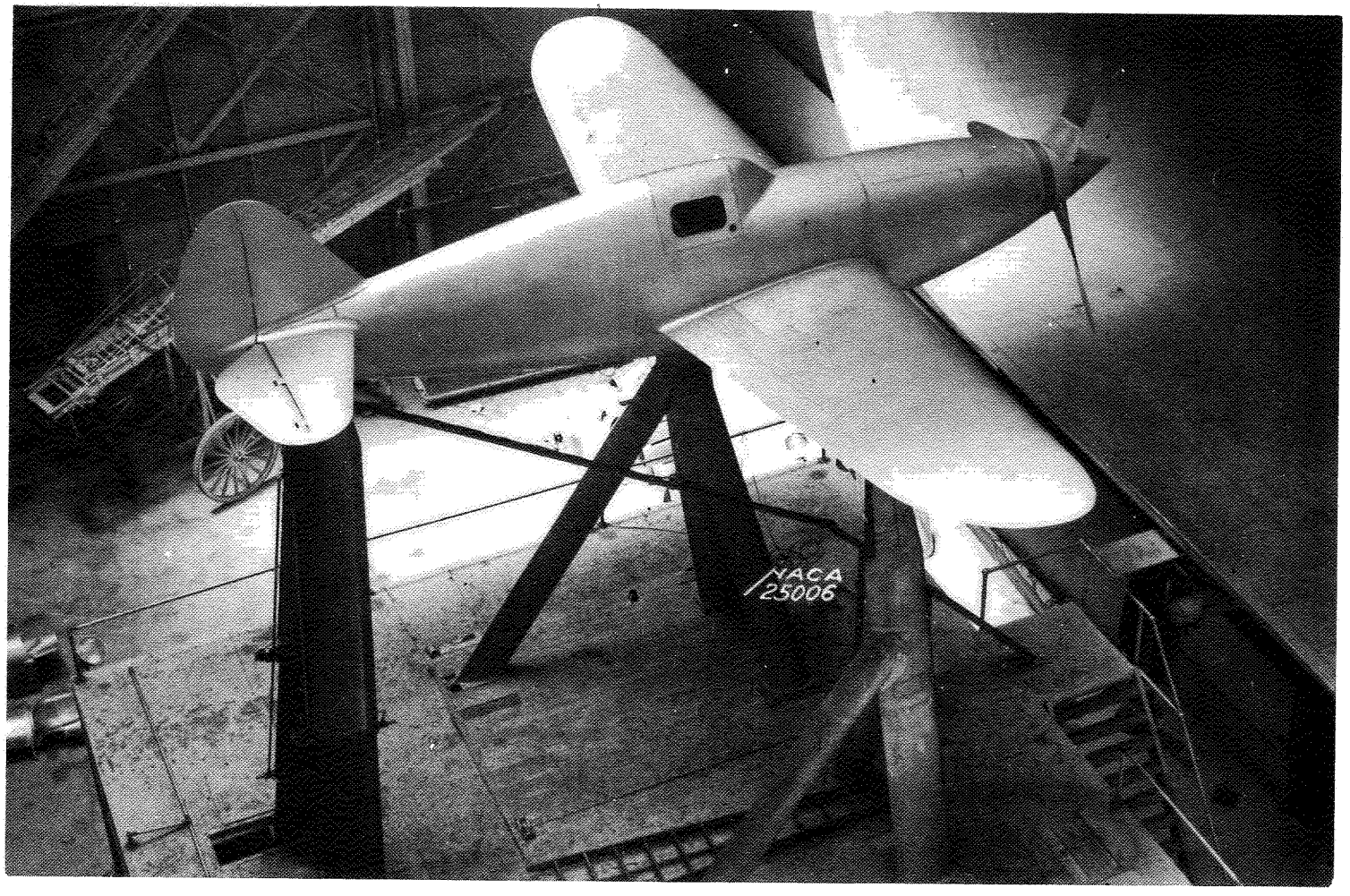

Figure 1.- Model mounted for tests in NACA full-scale tunnel.

Figure 2.-General arrangement of wind-tunnel model.

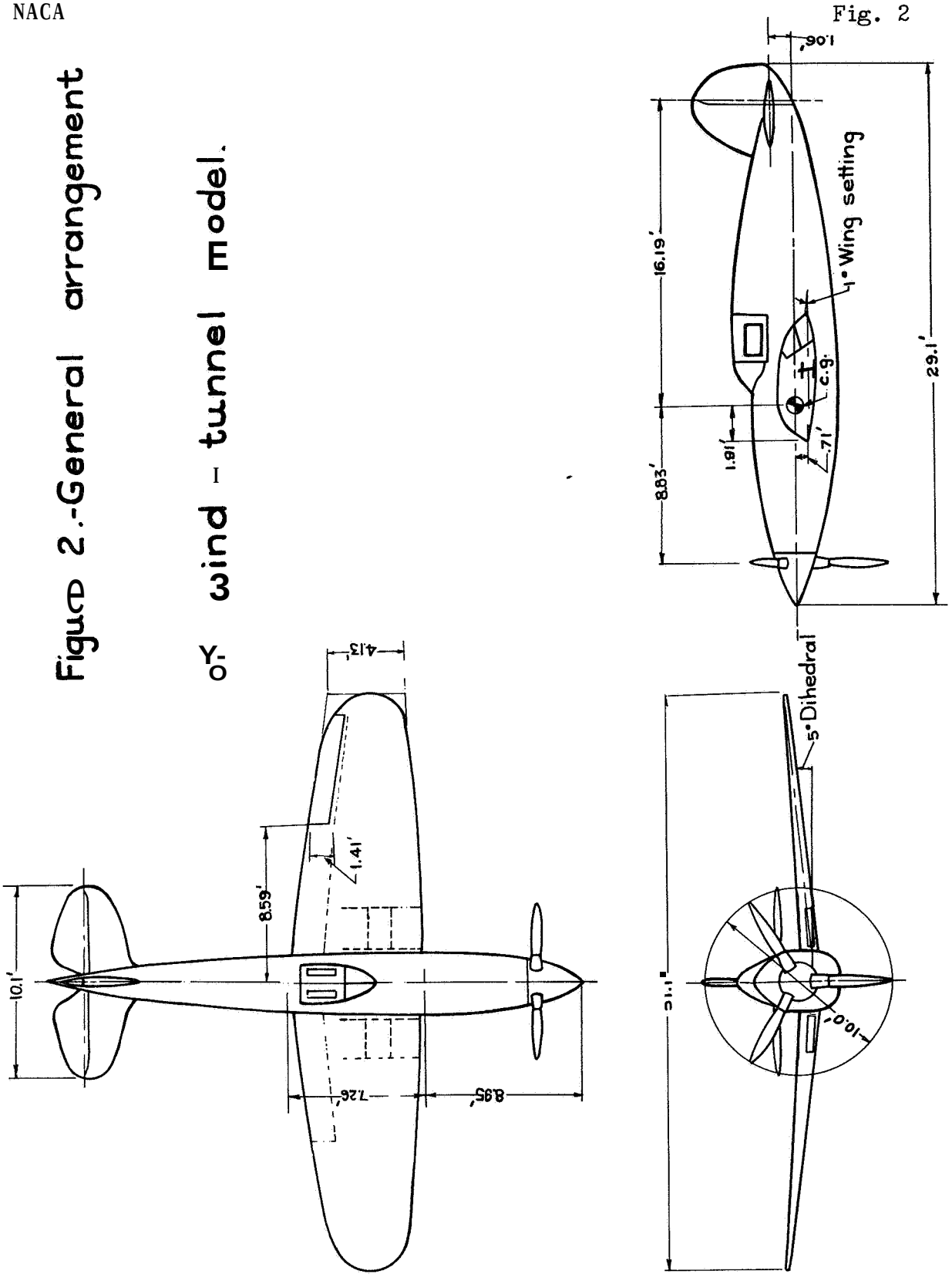

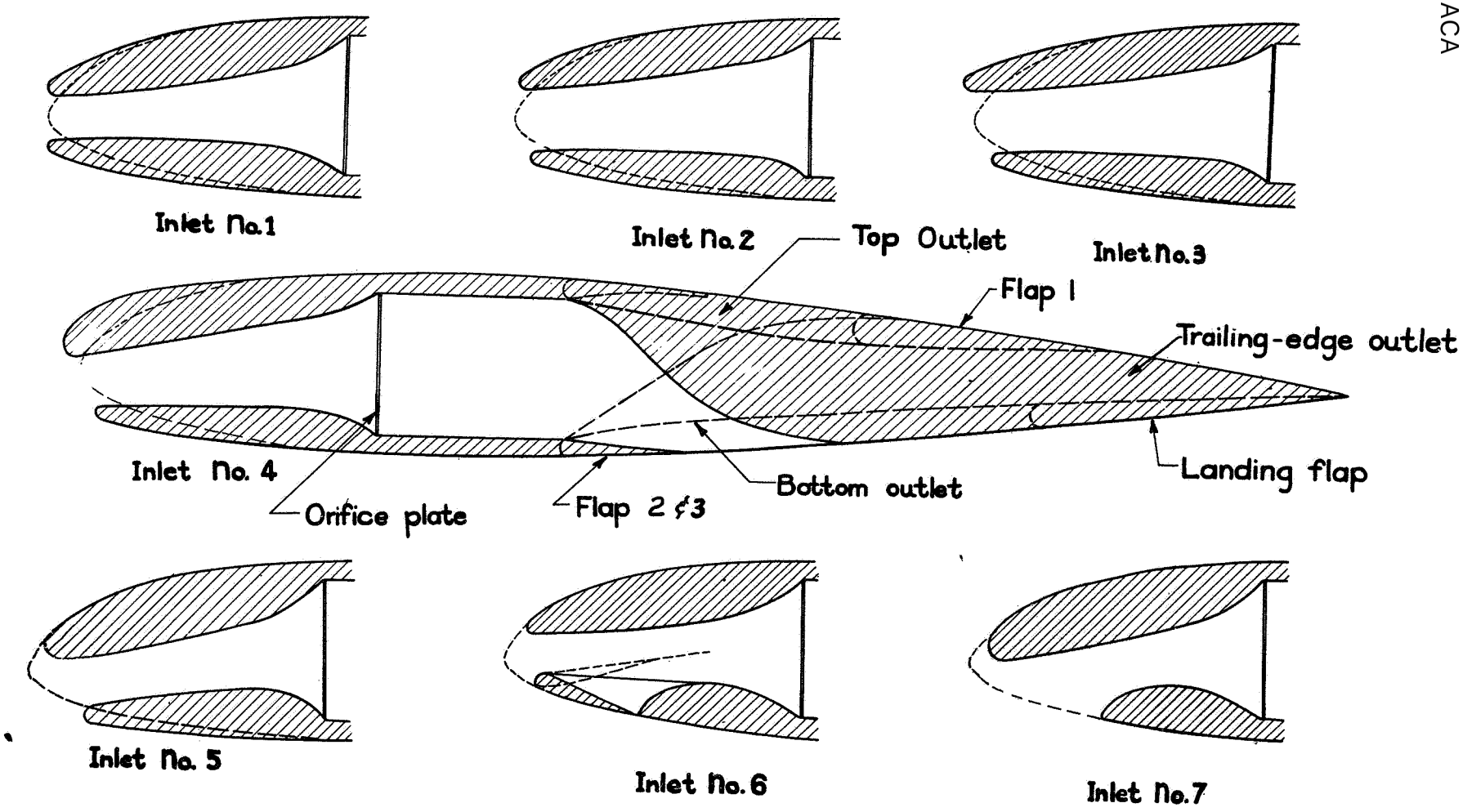

Figure 3.-Inlet and diffuser profiles.

L-401

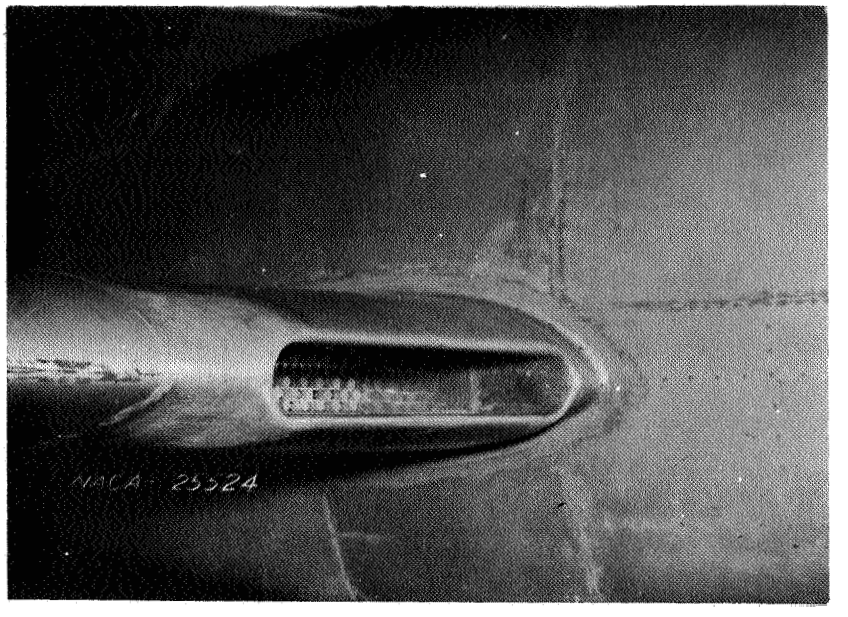

(a) Inlet 2.

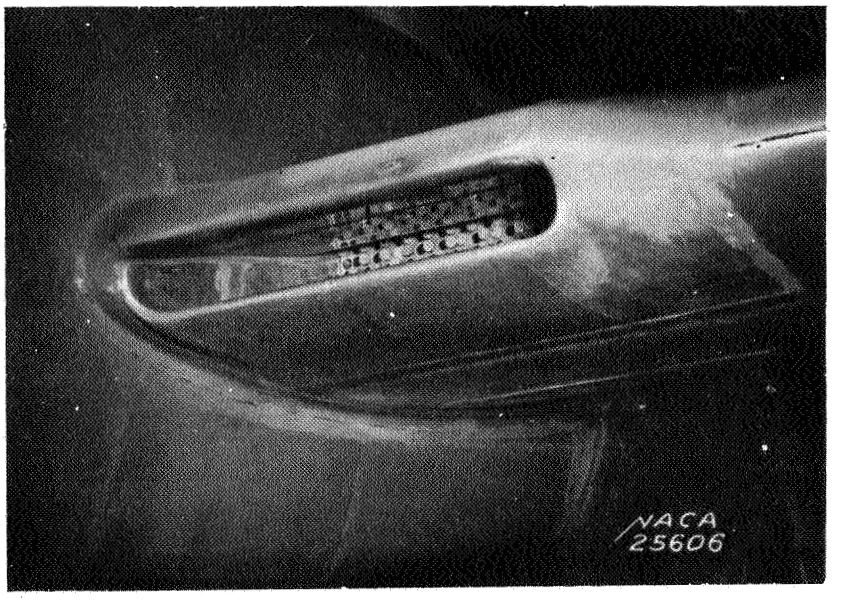

(b) Inlet 4.

Figure 4.- Typical duct inlets in leading edge of wing.

L407

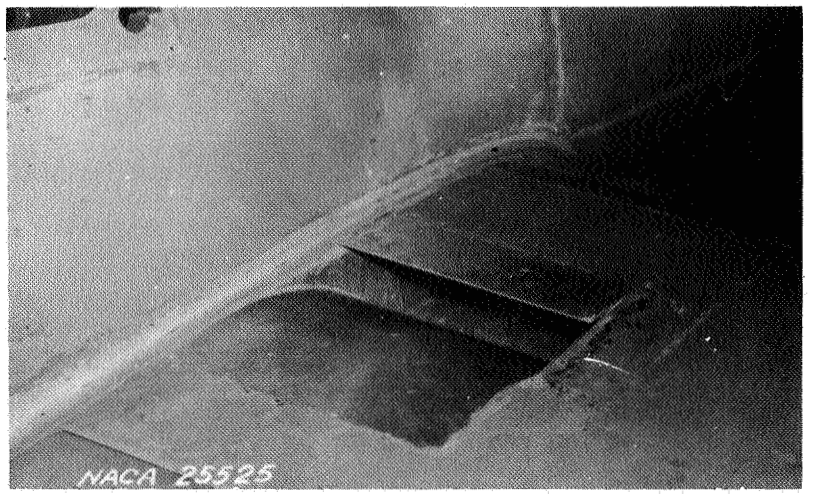

(a) In upper surface of wing.

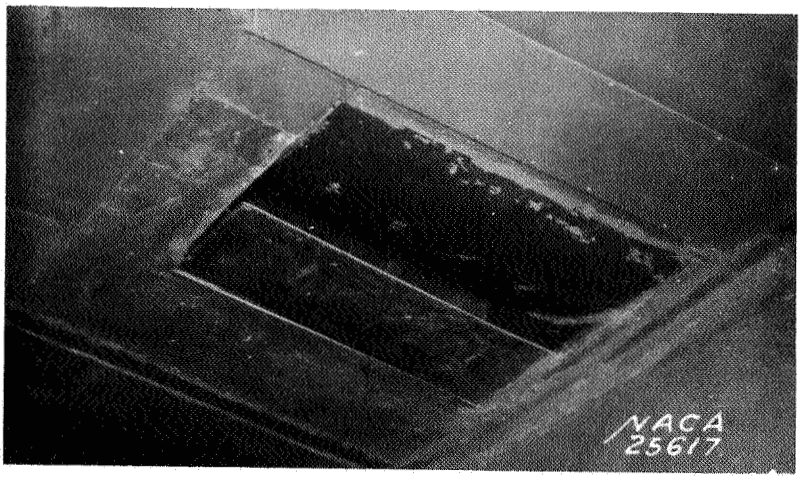

(b) In lower surface of wing.

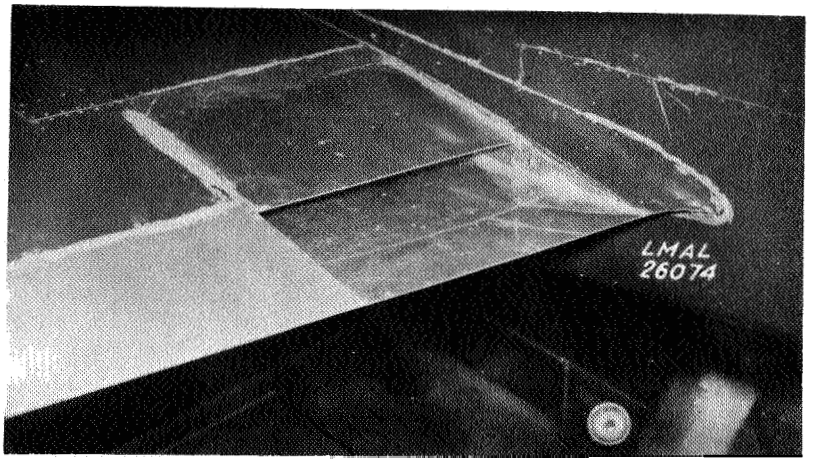

(c) In trailing edge of wing.

Figure 5.- Duet outlets.

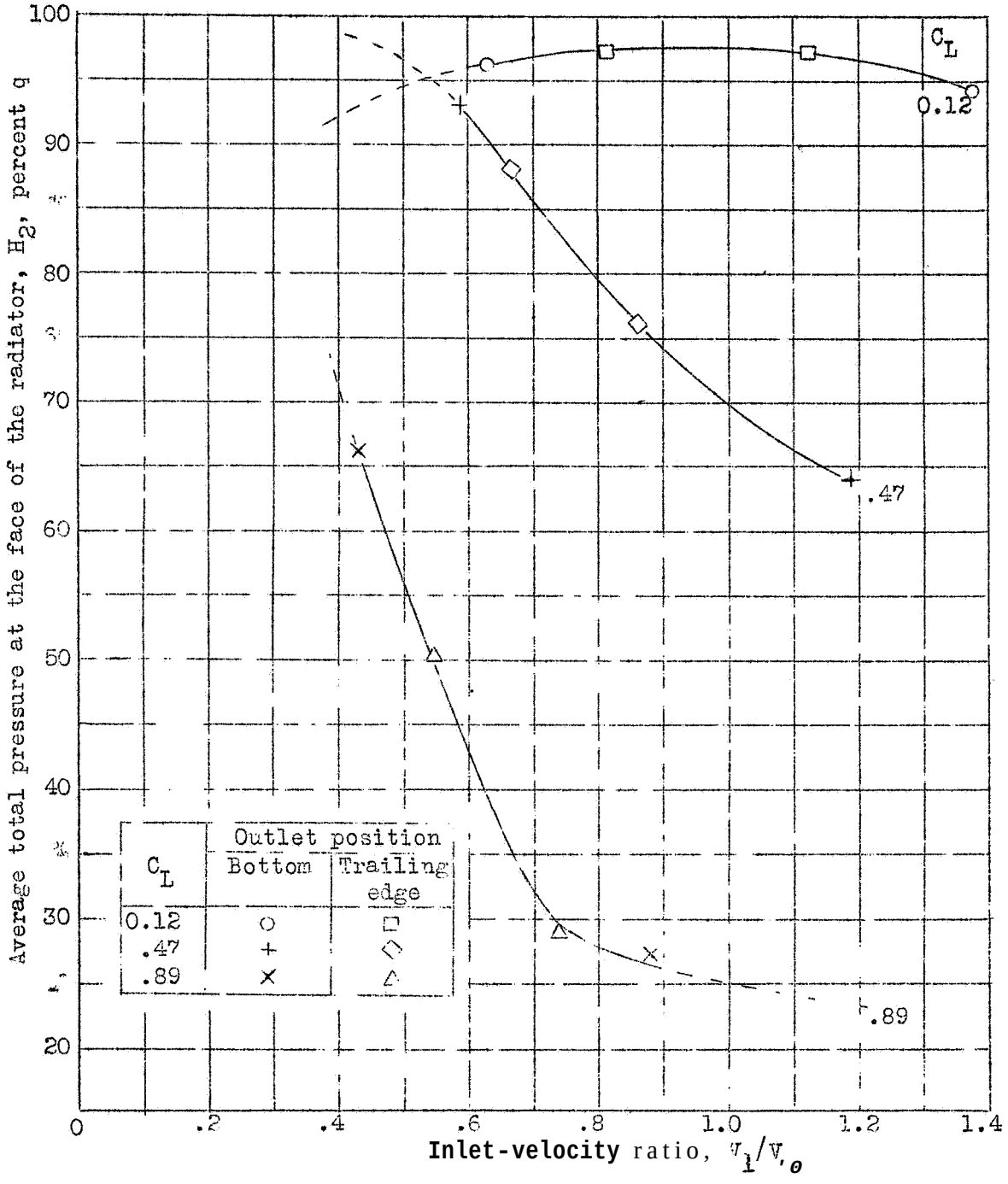

Figure 6.- Effect of inlet-velocity ratio on the average total pressure at the face of a radiator behind inlet 4. Propeller removed; airspeed, 63 miles per hour.

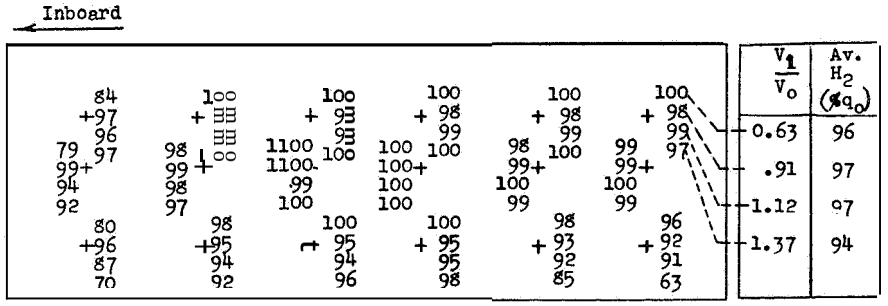

(a) $C_L = 0.12$

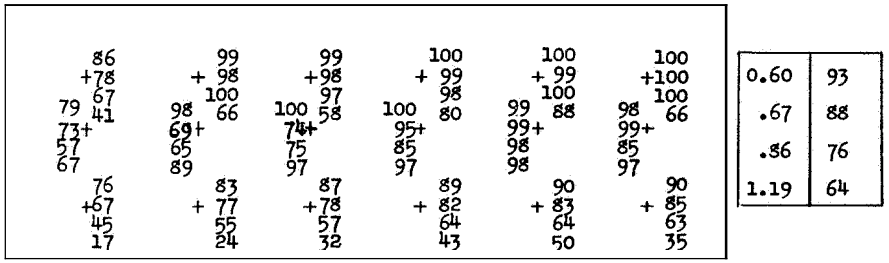

(b) $C_L = 0.47$.

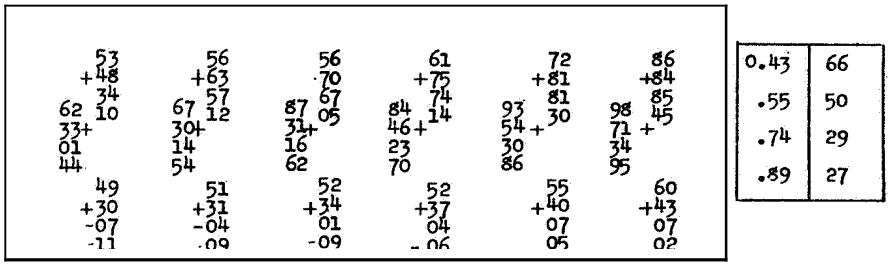

(c) $C_L = 0.89$.

Figure 7. - Effect of inlet-velocity ratio and lift coefficient on the pressure distribution at the face of a radiator behind inlet 4. Propeller removed; airspeed, 63 miles per hour. (Location of tube designated +.)

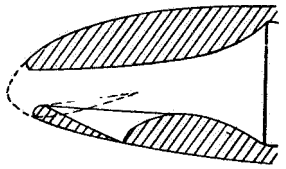

Inlet No. 6

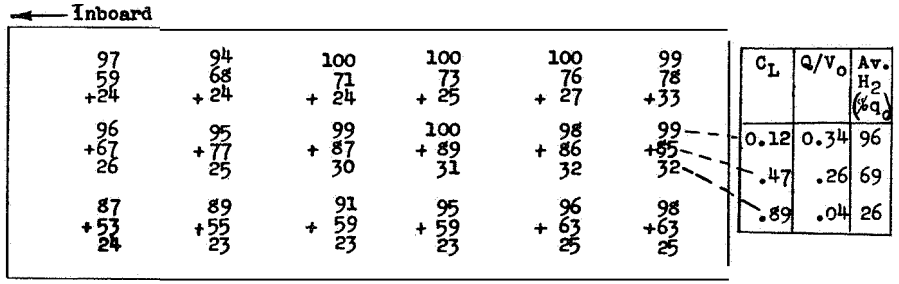

(a) Inlet flap closed.

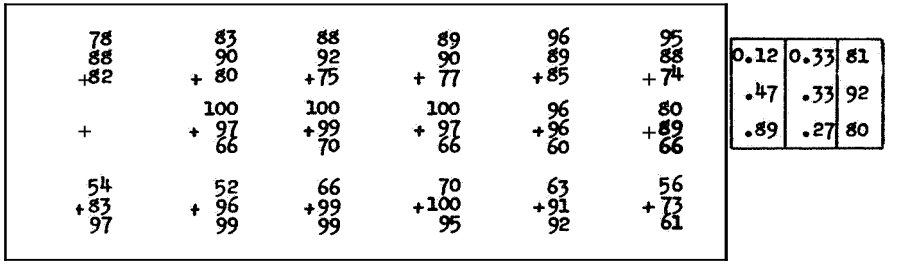

(b) Inlet flap open.

Figure 13. - Effect of inlet-flap position on the pressure-distribution recovery at the face of a radiator as a function of lift coefficient. Inlet 6; bottom outlet; outlet flaps closed; propeller removed. (Location of tube designated +.)

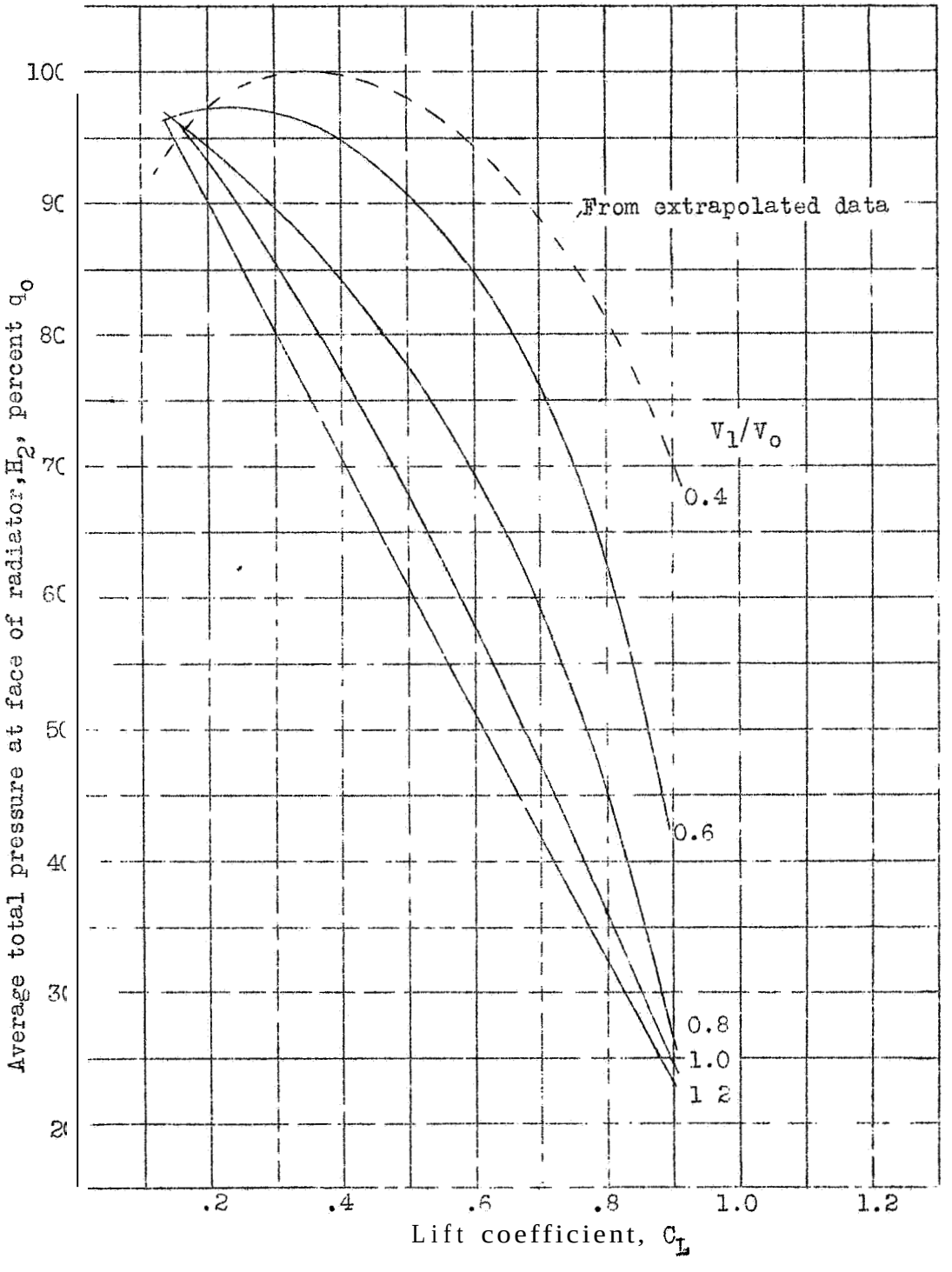

Figure 8.- Effect of lift coefficient on the average total pressure at the face of a radiator behind inlet 4. Propeller removed; airspeed, 63 miles per hour. (Cross plot of fig.6.)

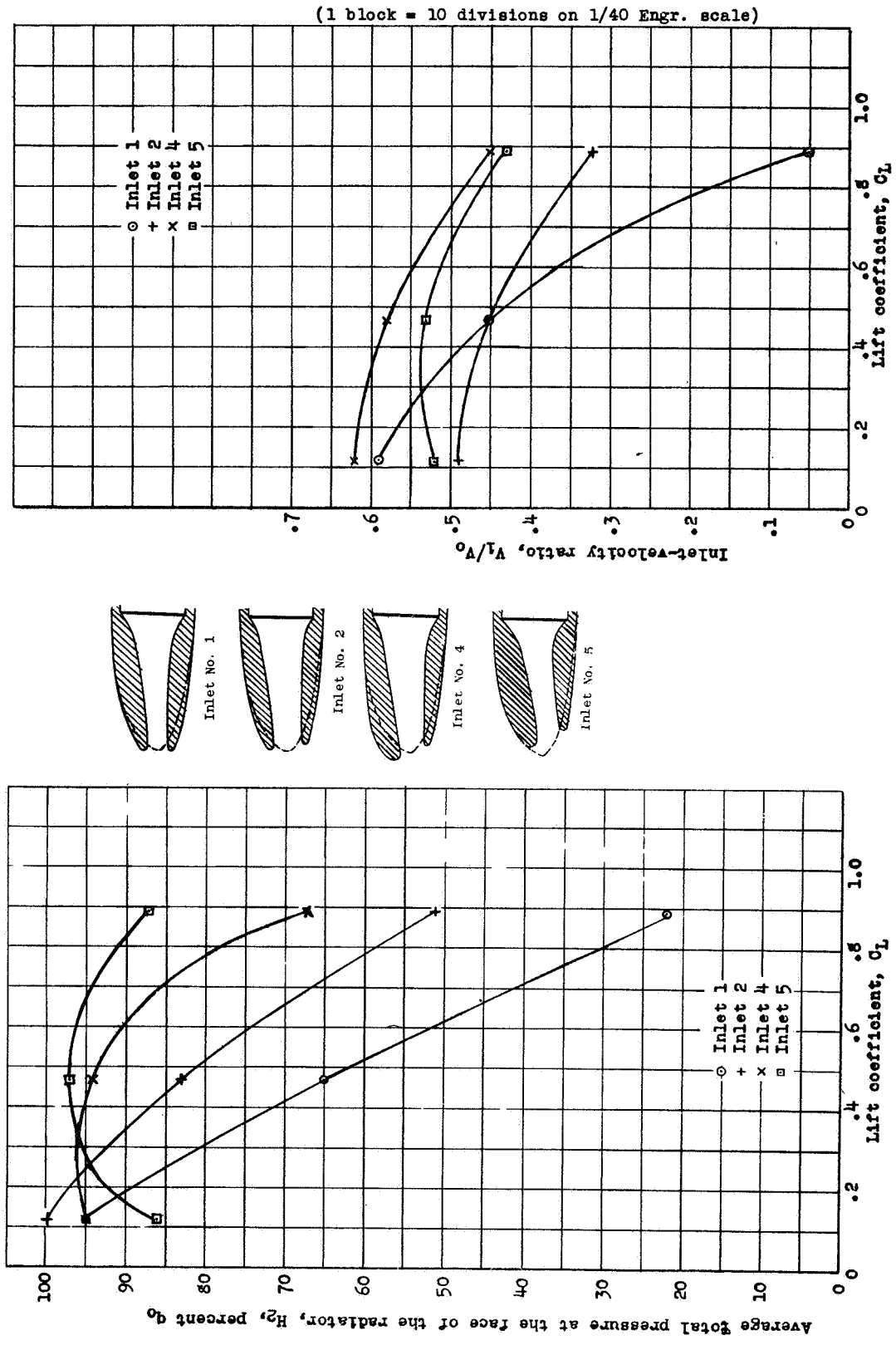

(a) Total pressure recovery.

(b) Inlet-velocity ratio.

Figure 9. - Effect of lift coefficient on the average total pressure at the face of the radiator behind inlets 1, 2, 4, and 5. Propeller removed; bottom flaps closed; $\Delta p/q_2$, 5.8.

L-407

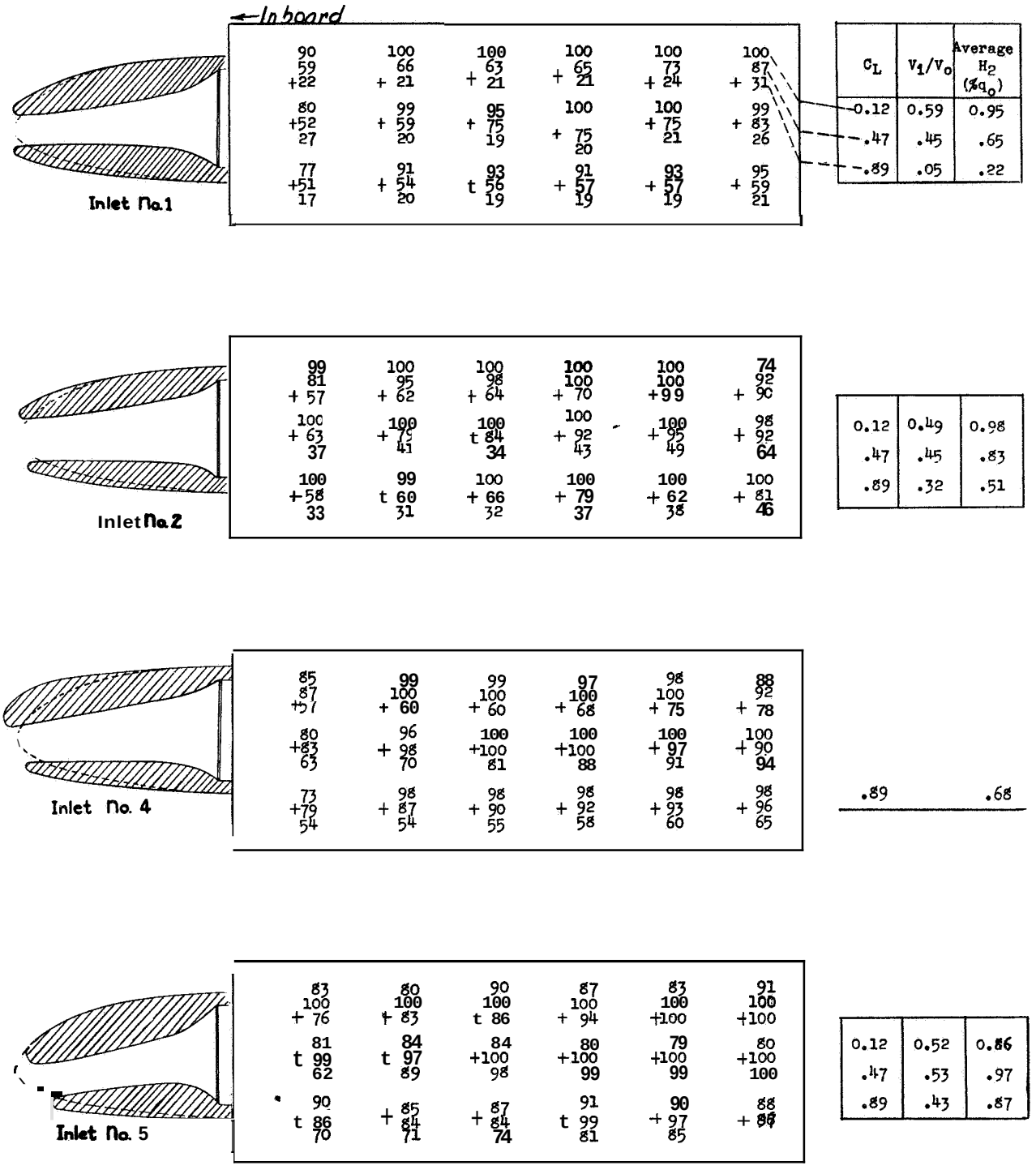

Figure 10. - Effect of lift coefficient on the total pressure distribution at the face of radiators behind inlets 1, 2, 4, and 5. Propeller removed; bottom cutlet; outlet flaps closed; $\Delta p/q_2$, 58. (Location of tube designated +.)

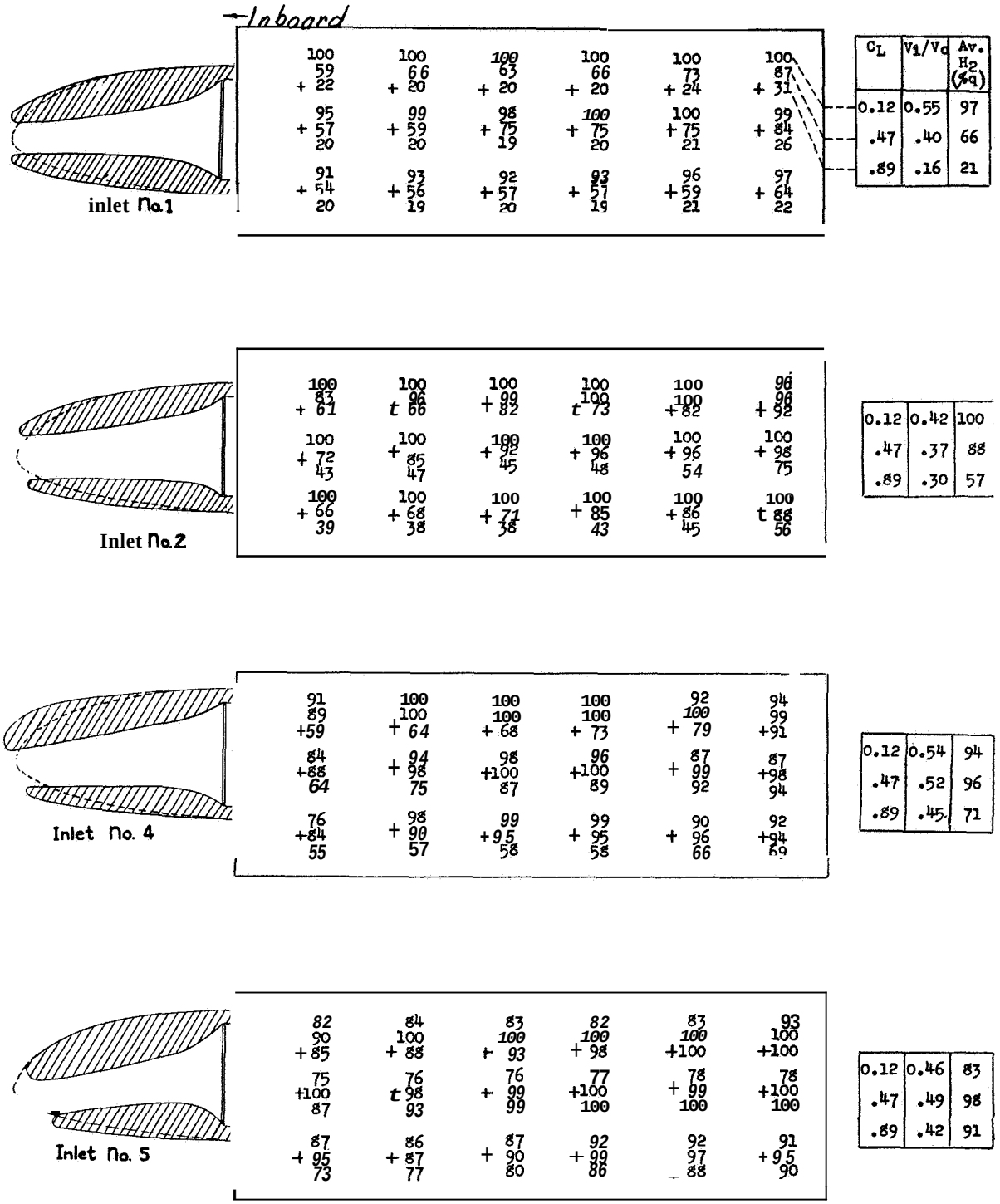

Figure 11. - Effect of lift coefficient on the total pressure distribution at the face of radiators behind inlets 1, 2, 4, and 5 Propeller removed; bottom outlet; outlet flaps closed; $\Delta p/q_0$, 11.0. (Location of tube designated +.)

L-407

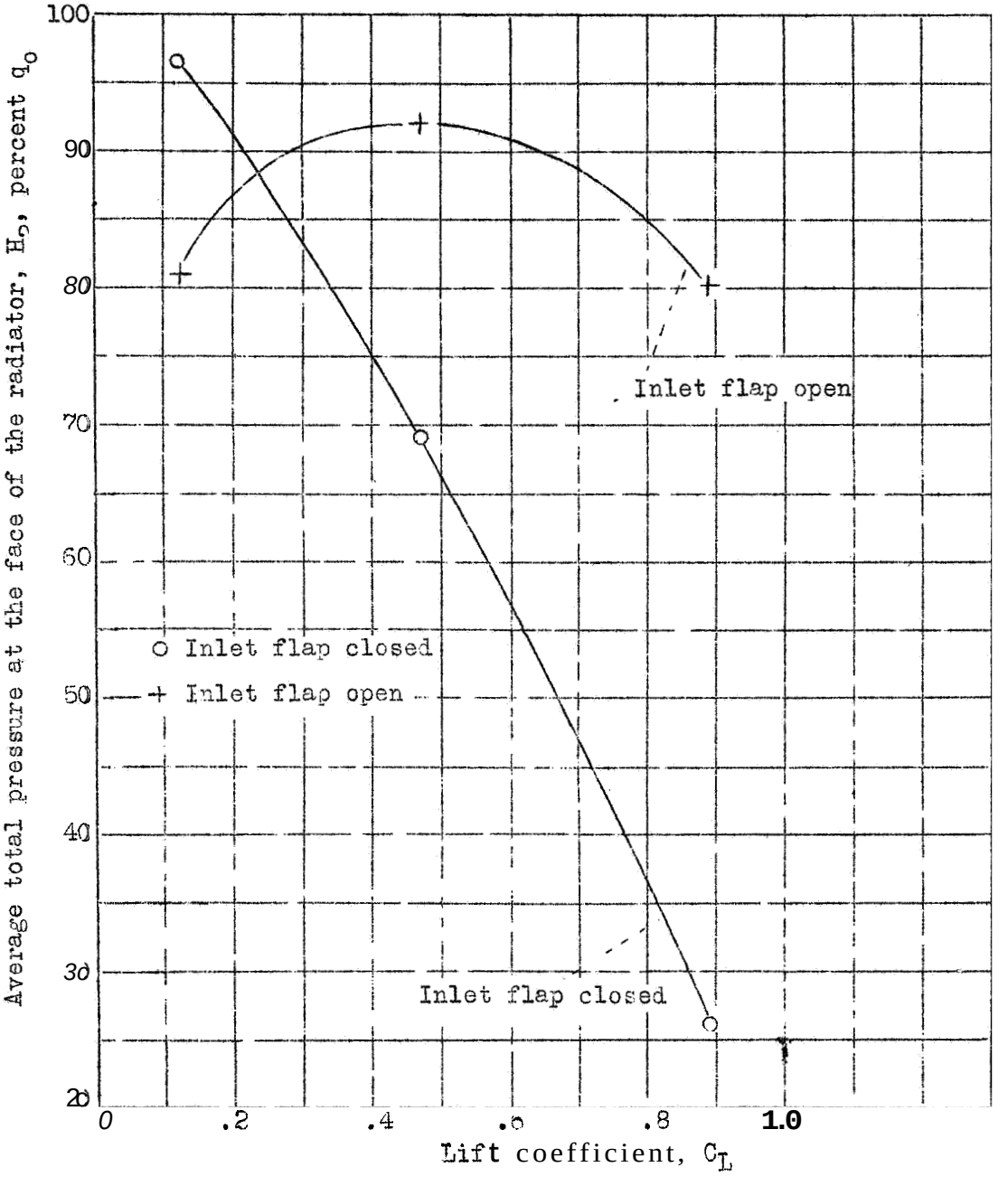

Figure 12.- Effect of inlet-flap position on the average total pressure at the face of the radiator as a function of lift coefficient. Inlet 6; bottom outlet; outlet flap closed; propeller removed.

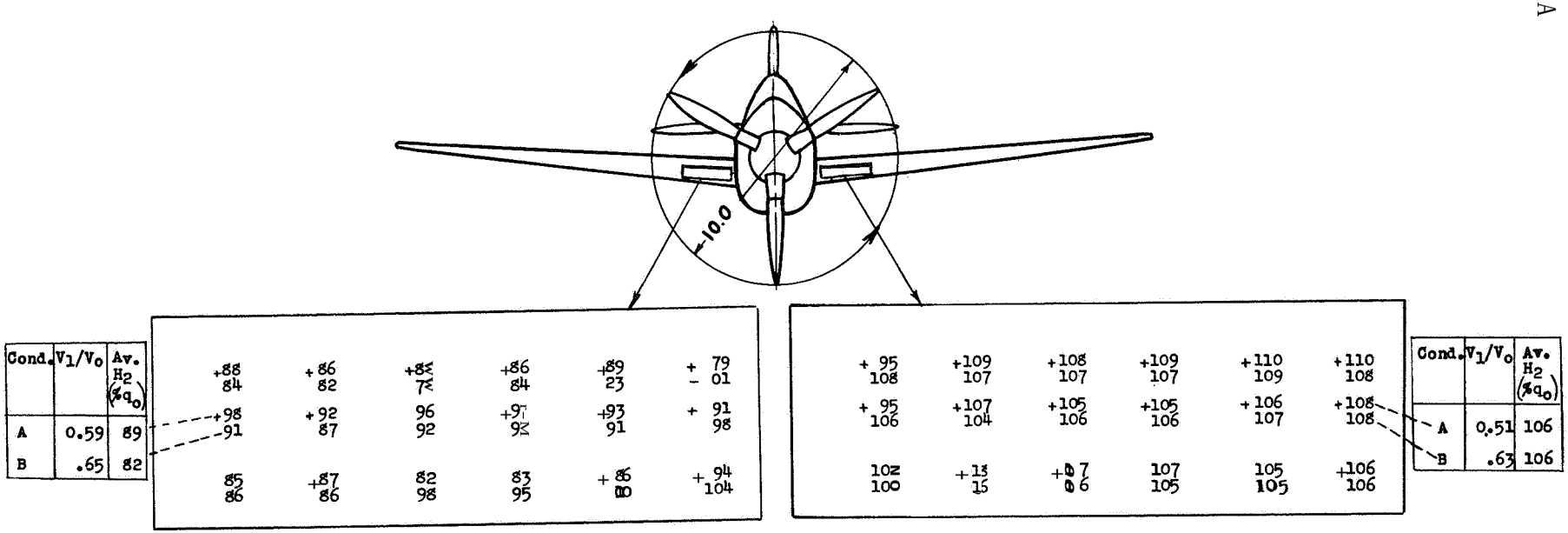

(a) $\Delta p/q_2 = 5.8$.

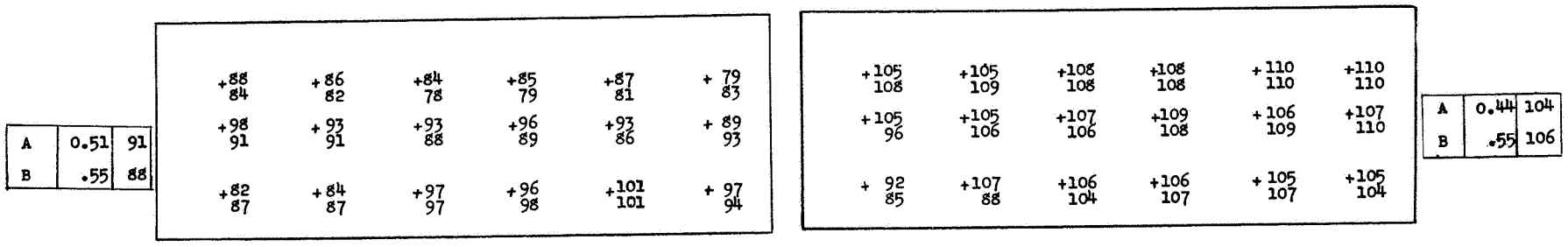

(b) $\Delta p/q_2 = 11.0$.

Figure 14. - Effect of propeller slipstream on the pressure recovery at the face of radiators symmetrically installed in the right and left wings. Inlet 4; bottom outlet; flaps closed; C_L, 0.12; β, 60°; T_c, 0.02. Condition A, outlet flap 3; condition B, outlet flap 2. (Location of tube designated +.)

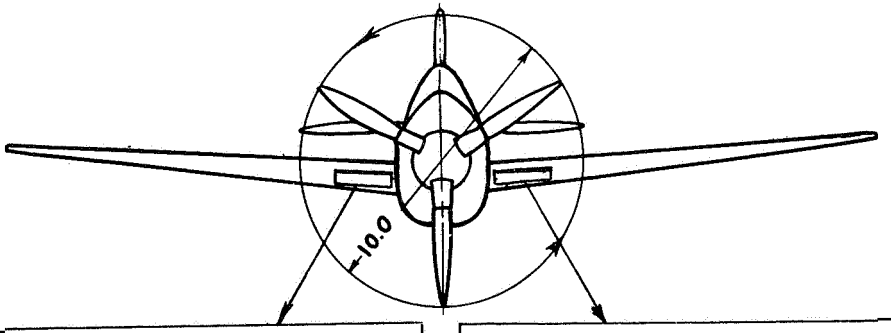

Cond.	V_1/V_o	Av. H_2 ($\%q_o$)
A	1.37	126
B	1.39	131

+146 154	+151 154	+146 164	+141 141	+143 146	+129 133
+147 151	+151 153	+148 150	+135 138	+137 140	+ 99 123
+	+114 114	+ 98 98	+108 110	+ 82 83	+ 74 74

+ 54 50	+ — 88	+ 72 83	+ 83 97	+114 —	+ 96 95
+ 78 117	+104 115	+113 117	+113 125	+126 135	+130 135
+ 21 18	+ 39 40	— 18	+ 55 53	+ 57 53	+ 47 52

Cond.	V_1/V_o	Av. H_2 ($\%q_o$)
A	1.08	81
B	1.12	82

(a) $\Delta p/q_2 = 5.8$.

Cond.	V_1/V_o	Av. H_2 ($\%q_o$)
A	1.04	138
B	1.02	138

+148 145	+148 149	+143 140	+140 140	+140 140	+130 134
+151 147	+148 150	+143 145	+138 140	+138 137	+138 139
+	+120 131	+130 140	+132 136	+130 119	+109 116

+ 80 96	+102 102	+107 102	+126 112	+ 124	+122 125
+ 92 104	+113 117	+122 122	+127 128	+133 134	+135 135
+ 46 50	+69 73	+ 77 79	+ 85 86	+ 85 84	+ 80 81

Cond.	V_1/V_o	Av. H_2 ($\%q_o$)
A	0.89	100
B	.81	103

(b) $\Delta p/q_2 = 1.0$

Figure 15. - Effect of propeller slipstream on the pressure recovery at the face of radiators symmetrically installed in the right and left wings. Inlet 4; bottom outlet; flaps open; C_L, 0.47; β, 40°; T_c, 0.11. Condition A, outlet flap 3; condition B, outlet flap 2. (Location of tube designated +.)

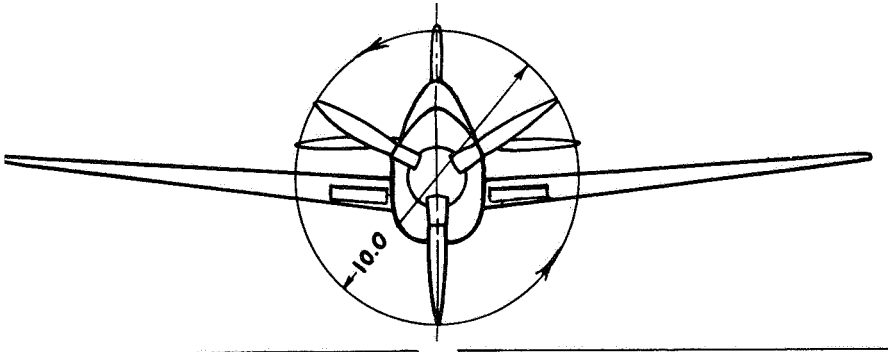

Cond.	V_1/V_o	Av. H_2 ($\%q_o$)
C	0.59	97
D	.57	97

+95 85	+97 89	+ 98 94	+99 94	+ 98 88	+89 81
+ 98 96	+ 98 101	+ 91 111	+100 106	97 94	+97 92
+ 98 108	+ 90 99	+ 96 109	+ 95 106	+ 9; 10 (N)	+93 93

+ 83 108	+ 99 107	+ 90 108	+ 87 109	+ 83 112	+ 91 110
+ 81 105	+ 84 106	+ 84 103	+ 80 107	+ 70 107	+ 79 107
+ 90 103	+ 85 106	87 105	+ 91 107	+ 90 105	+ 88 105

Cond.	V_1/V_o	Av. H_2 ($\%q_o$)
C	0.52	86
D	.51	107

(a) Outlet flap 3

+ 99 98	+ 99 91	+ 99 98	+100 103	+100 94	+98 87
+ 100 98	+100 101	+100 110	+100 108	+ 98 98	+100 104
+ 100 100	+ 88 100	+ 95 106	+ 95 105	+ 95 101	+ 89 112

+ 100 108	97 109	+ 97 108	+ 99 109	+ 90 111	+ 95 110
+ 90 106	+ 90 103	+ 91 98	+ 90 107	+ 81 107	+ 80 107
+ 99 103	+ 86 105	+ 80 103	+ 98 103	+ 41 44	+ 90 99

C	0.62	98
D	.66	101

C	0.62	92
D	.61	106

(b) Outlet flap 2.

Figure 16. - Effect of propeller slipstream on the pressure recovery at the face of radiators symmetrically installed in the right and left wings. Inlet 5, bottom outlet, flaps closed; $\Delta p/q_o$, 5.8; C_L, 0.12. Condition C, propeller removed; condition D, $\beta = 60^\circ$ and $T_c = 0.02$. (Location of tube designated +.)

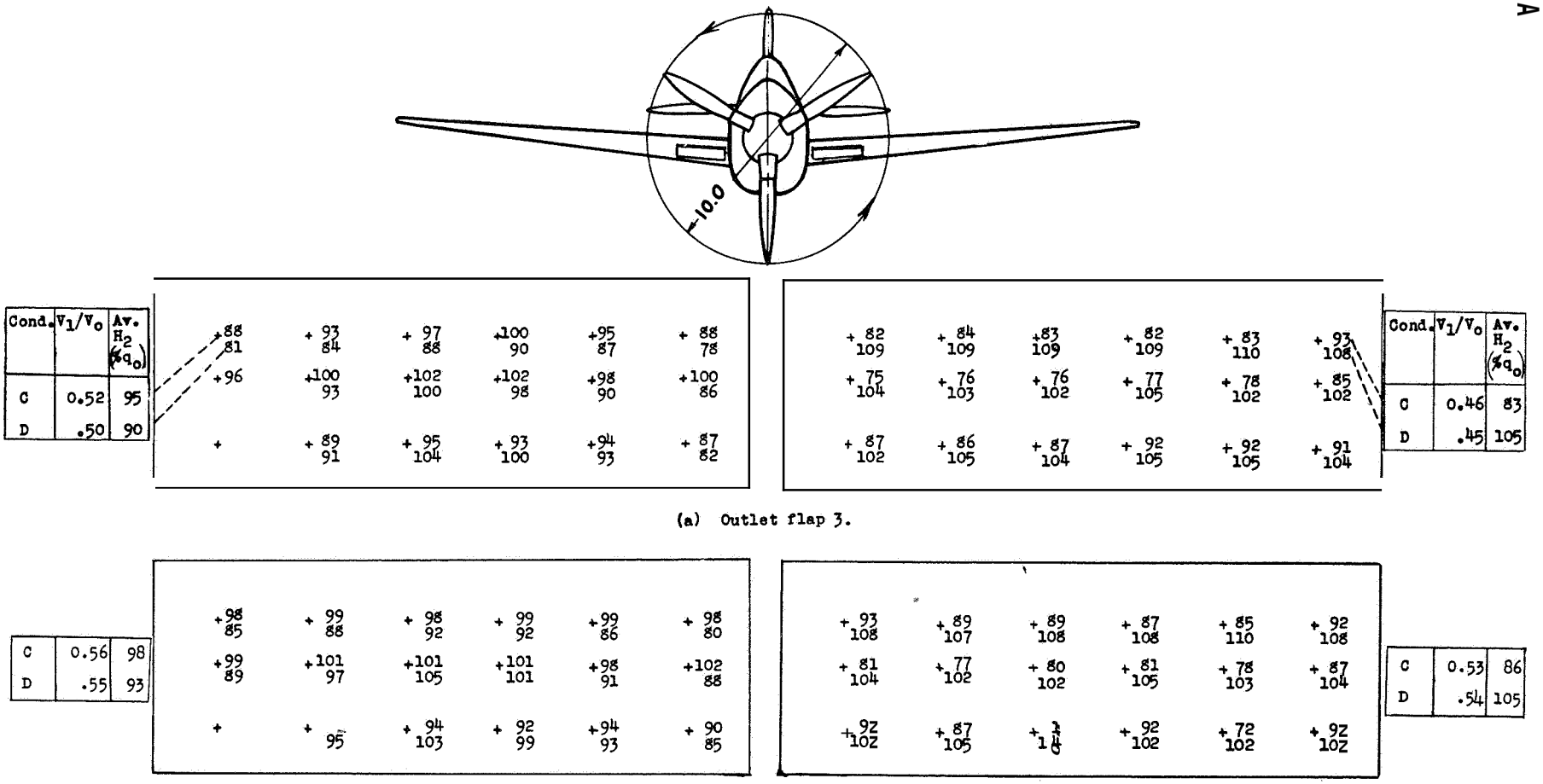

(a) Outlet flap 3.

(b) Outlet flap 2.

Figure 17. - Effect of propeller slipstream on the pressure recovery at the face of radiators symmetrically installed in the right and left wings. Inlet 5; bottom outlet; flaps closed; $\Delta p/q_2$, 11.0; C_T, 0.12. Condition C, propeller removed; condition D, $\beta = 60^{\circ}$ and $T_c = 0.02$. (Location of tube designated +)

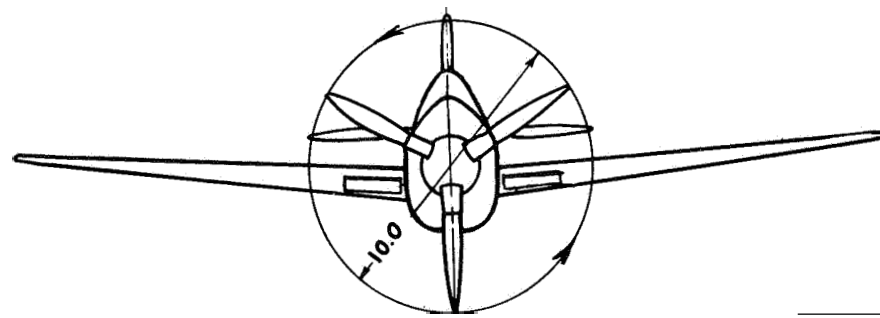

Cond.	V_1/V_o	Av. H_2 ($\%q_o$)
C	0.98	88
E	1.78	133

99 148	+100 148	+ 98 100	+ 99 143	+ 99 141	+100 143
+100 149	+100 151	+100 148	+100 145	+ 97 137	+100 143
	+ 54 140	+ 68 122	+ 56 104	+ 66 100	+ 54 92

+100 135	+100 130	+100 134	+100 137	+100 142	+100 142
+ 93 132	+ 94 132	+ 99 127	+100 134	+ 98 135	+ 98 135
+	+ 41 105	+ 36 90	+ 37 89	+ 38 100	+ 67 106

Cond.	V_1/V_o	Av. H_2 ($\%q_o$)
C	1.08	84
E	2.03	124

(a) Outlet flap 3

Cond.	V_1/V_o	Av. H_2 ($\%q_o$)
C	1.11	88
E	1.79	147

+ 99 153	+ 99 151	+ 99 145	+ 98 145	+ 98 145	+ 98 143
+100 153	+100 155	+100 151	+100 148	+ 97 143	+ 99 148
+	+ 92 142	+ 71 143	+ 65 171	+ 49 130	+ 48 135

+100 137	+100 134	+ 97 134	+100 137	+100 142	+100 144
+ 94 134	+ 95 130	+ 98 129	+100 135	+ 98 135	+ 99 135
	+ 41 102	+ 37 94	+ 32 90	+ 29 92	+ 73 109

Cond.	V_1/V_o	Av. H_2 ($\%q_o$)
C	1.11	82
E	1.93	123

(b) Outlet flap 2

Figure 18. - Effect of propeller slipstream on the pressure recovery at the face of radiators symmetrically installed in the right and left wings. Inlet 5; bottom outlet; flaps open; $\Delta p/q_o$, 5.8; C_L, 0.47. Condition C, propeller removed; condition E, $\beta = 40^\circ$ and $T_c = 0.11$. (Location of tube designated +.)

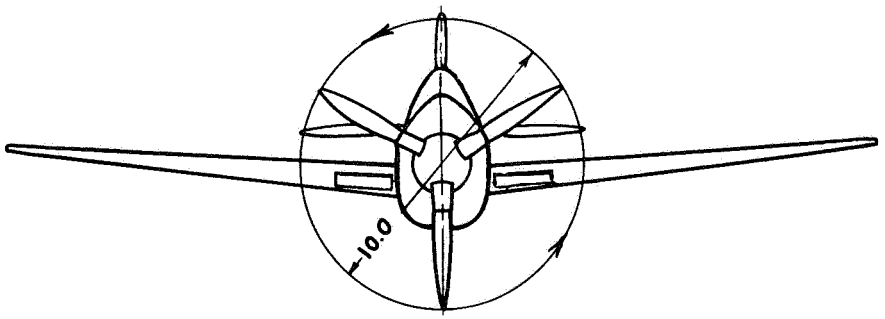

Cond.	V_1/V_0	Av. H_2 ($\%q_0$)
C	0.90	94
E	1.50	151

+99 149	+99 149	+98 140	+100 142	+99 140	+99 144
+100 150	+100 153	+100 150	+100 147	+98 139	+100 147
+	+75 137	8 12	+81 13	+80	+79

+100 13	+100 13	+100 131	+100 136	10 13	+100 141
+98 134	+96 128	+100 12	+100 134	+9 13	+
100	+75 85	+6 8		+	+8 110

Cond.	V_1/V_0	Av. H_2 ($\%q_0$)
C	0.86	95
E	1.68	121

(a) Outlet flap 3.

C	0.78	93
E	1.61	142

+97 148	+100 150	+100 148	+100 142	+100 140	+100 140
+100 152	+99 152	+99 149	+100 144	+96 139	+99 148
+	+70 138	+95 136	+80 121	+82 136	+75 131

+100 136	+100 134	+100 134	+100 136	+100 141	+100 141
+99 133	+96 129	+97 129	+100 136	+98 134	+
+101	+80 110	+73 104	+114	+74 118	+86 119

C	0.90	94
E	1.49	127

(b) Outlet flap 2

Figure 19. - Effect of the propeller slipstream on the pressure recovery at the face of radiators symmetrically installed in the right and left wings. Inlet 5; bottom outlet; flaps open; $\Delta p/q_2$, 11.0; C_L, 0.47. Condition C, propeller removed; condition E, $\beta = 40^\circ$ and $T_c = 0.11$. (Location of tube designated +.)

L-407

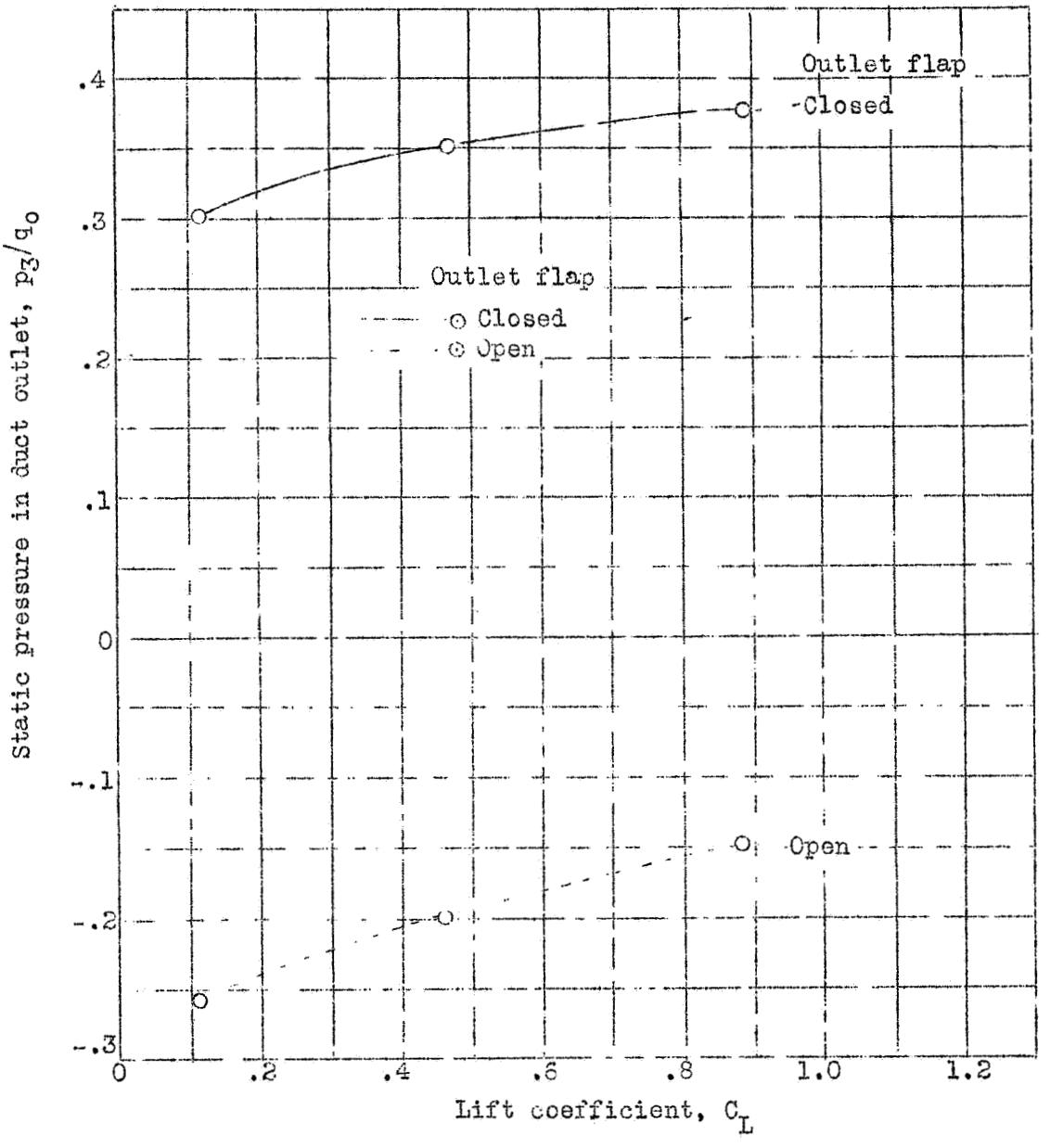

Figure 20.- Effect of outlet-flap deflection on the static pressure at an outlet in the lower surface of the wing as a function of lift coefficient* Propeller removed; inlet 4; $\Delta p/q_2$, 5.8.

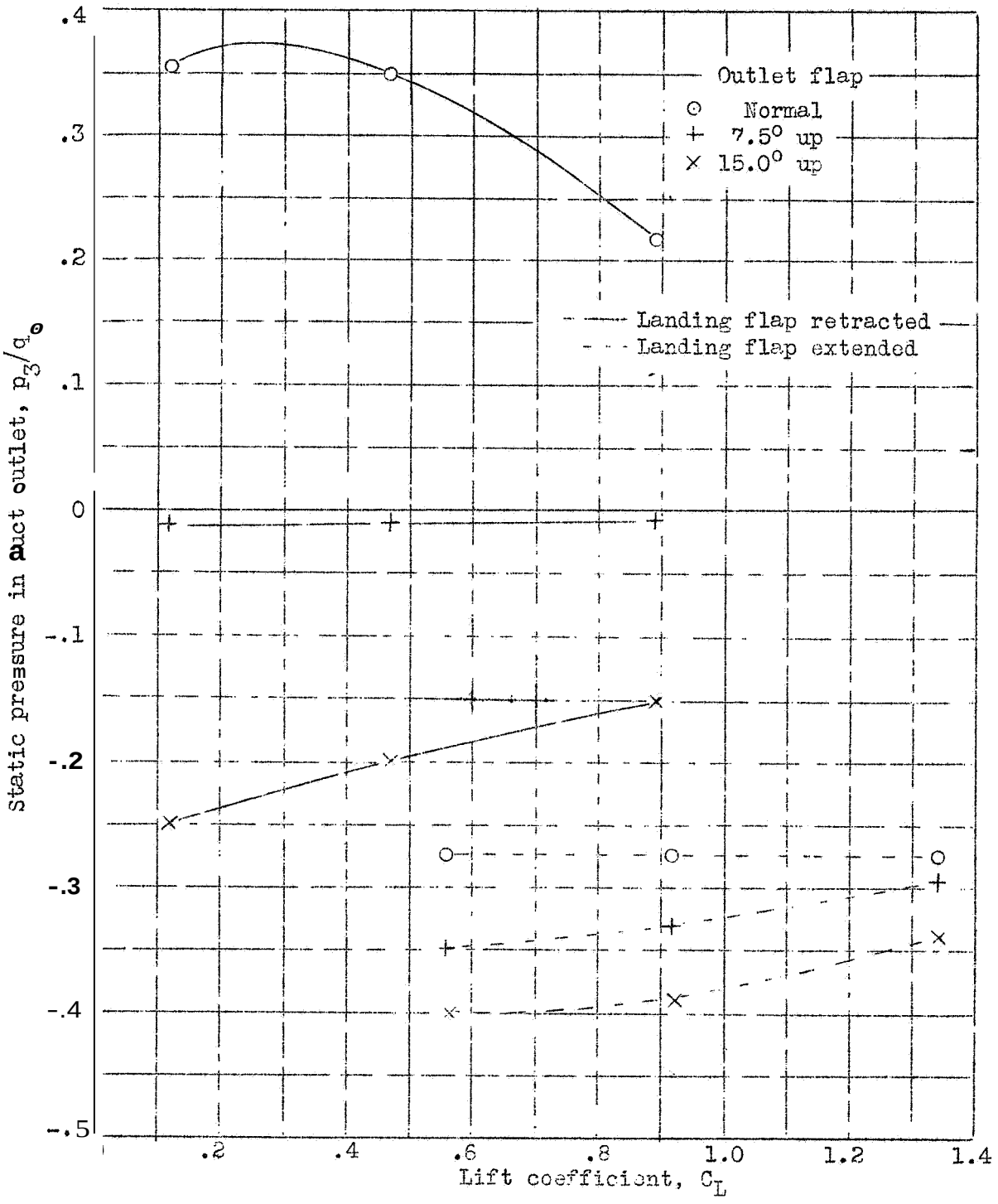

Figure 21.- Effect of flap deflection on the static pressure at an outlet over the trailing edge of the wing as a function of lift coefficient Propeller removed; inlet, 4; $\Delta p/q_2$, 5.8

L-407

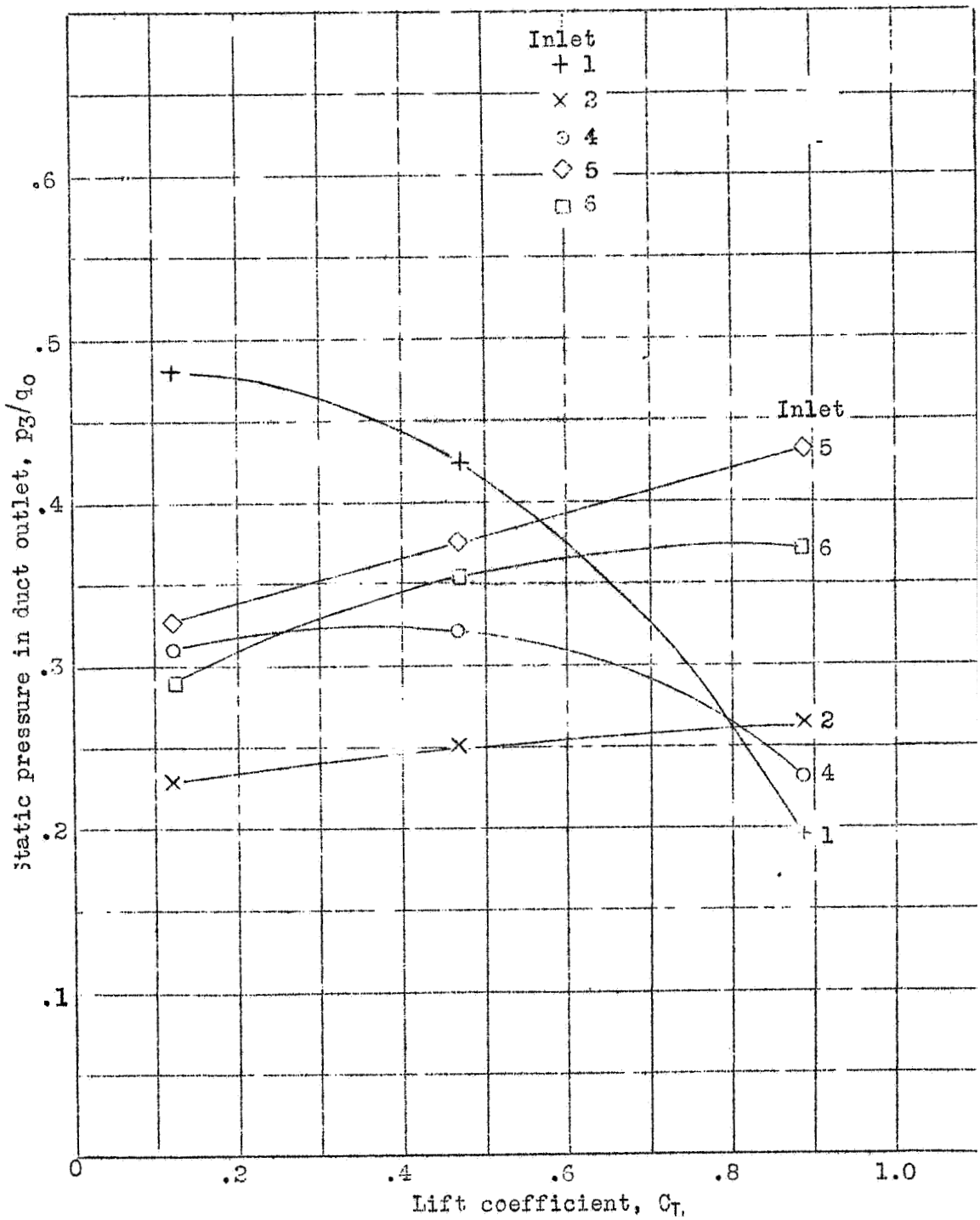

Figure 22.- Effect of inlet design of the static pressure at an outlot in the lower surface of a wing as a function of lift coefficient. Propeller removed,

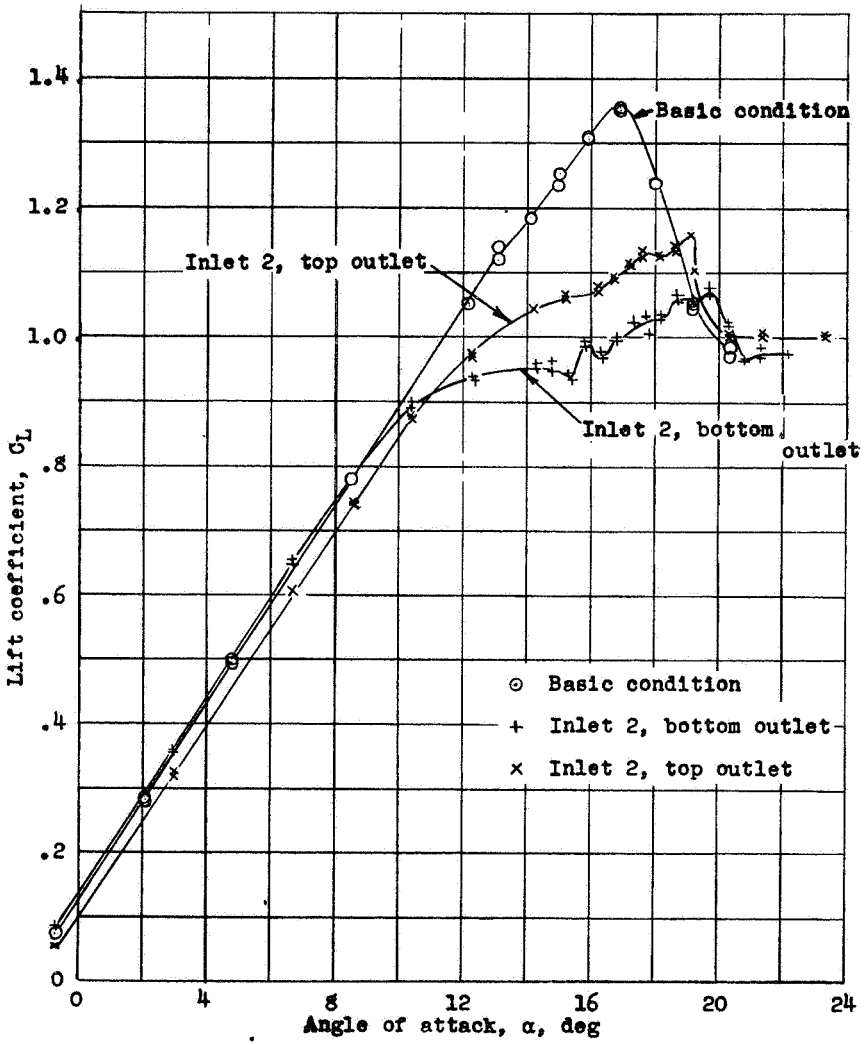

Figure 23. - Effect of outlet position on the maximum lift coefficient of the complete model with ducts installed in both wings. Propeller removed; landing flaps neutral; inlet 4; outlet flaps closed; $\Delta p/q_2$, 5.8.

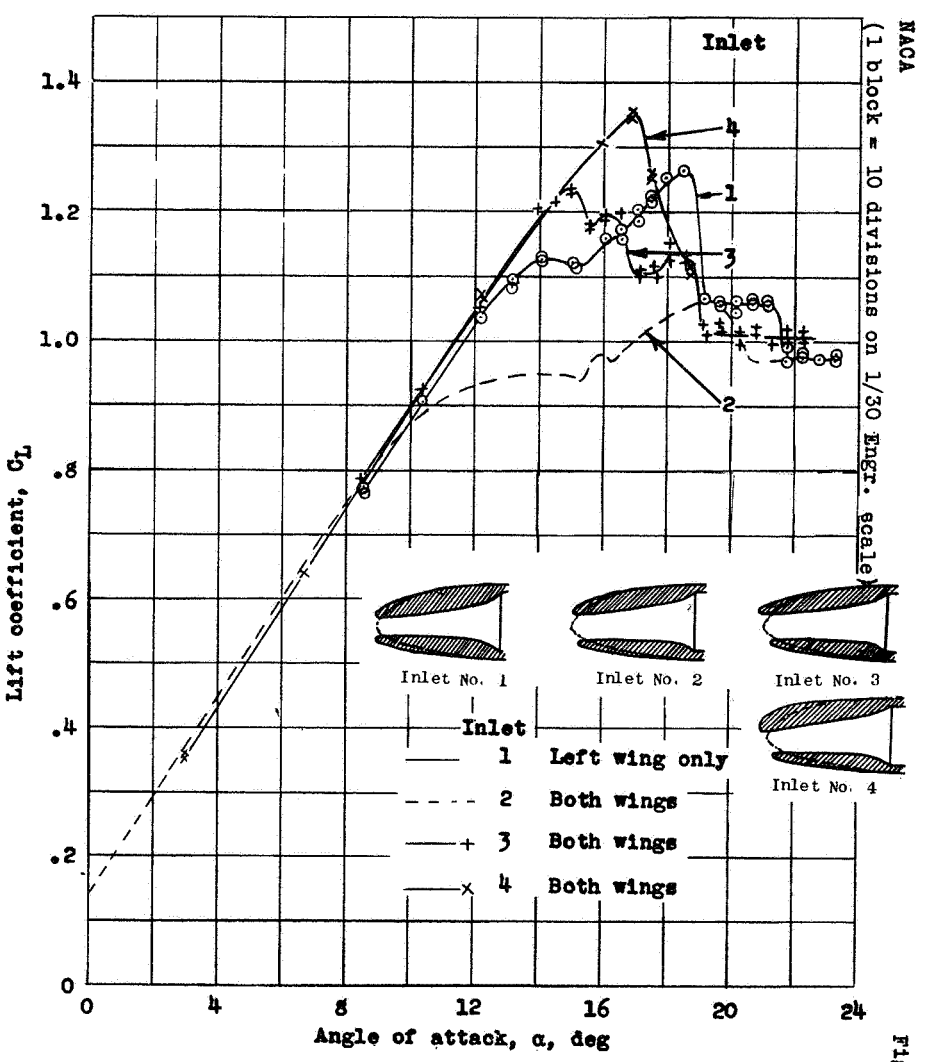

Figure 24. - Effect of inlet size and upper-lip position on the maximum lift coefficient of the complete model. Propeller removed; landing flaps neutral; bottom outlet; outlet flaps closed; $\Delta p/q_2$, 5.8.

Figs. 23,24

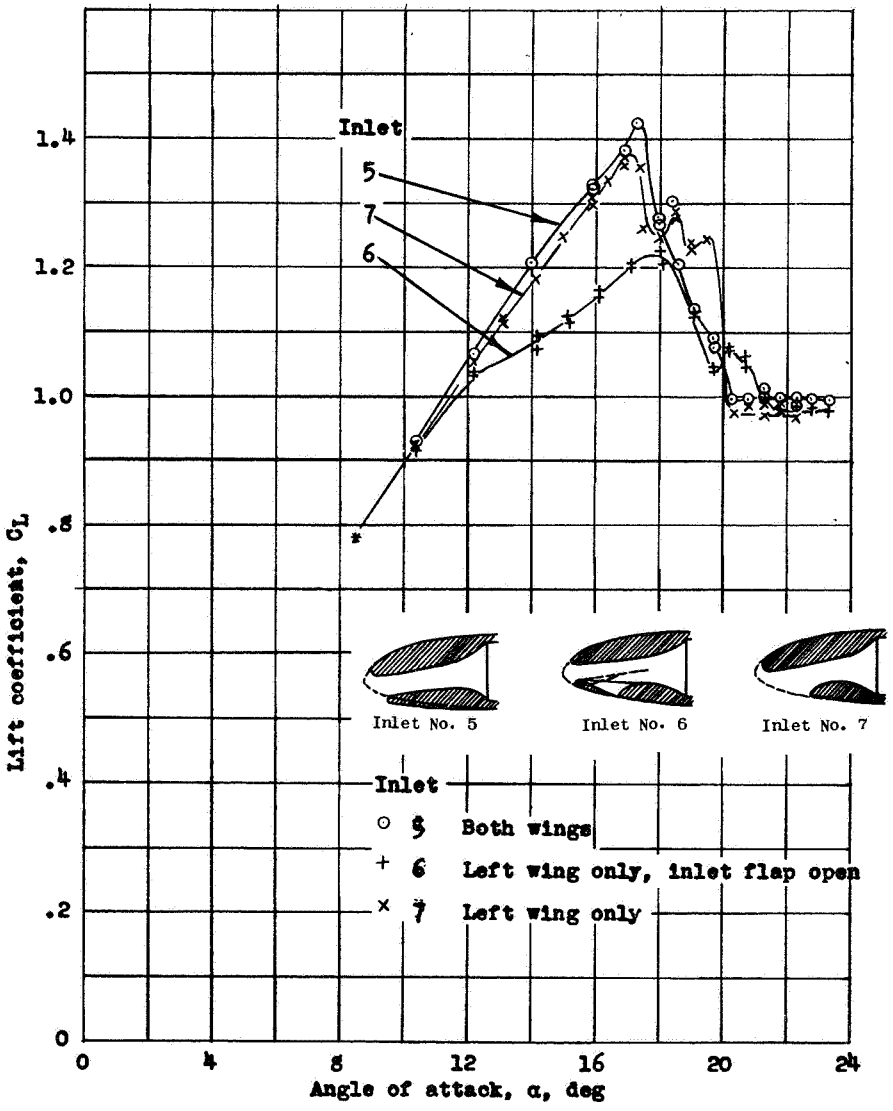

Figure 25. - Effect of lip position, leading-edge radius, and diffuser inclination on the maximum lift coefficient of the complete model. Propeller removed; landing flaps neutral; bottom outlet; outlet flaps closed; $\Delta p/q_2$, 5.8.

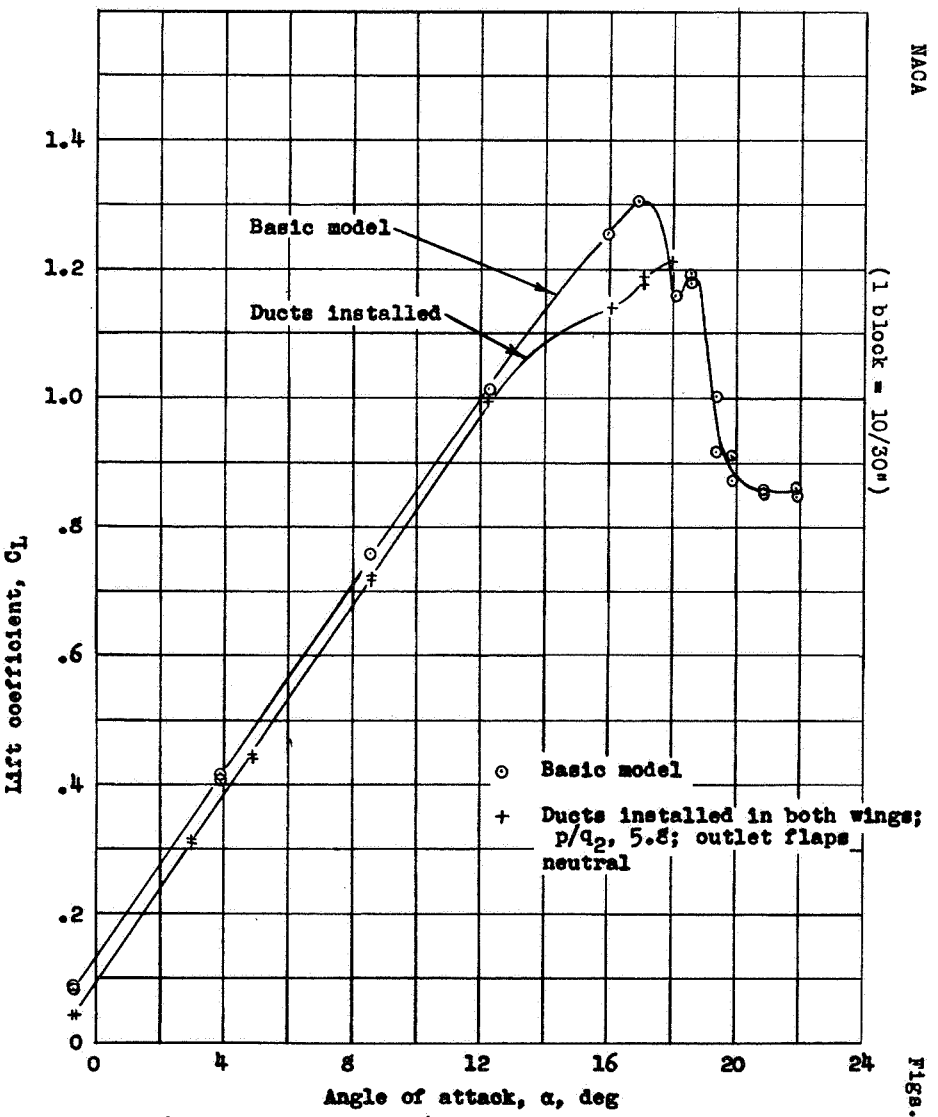

Figure 26. - Effect of inlet 4 and trailing-edge outlet on maximum lift coefficient of the model with tail surfaces removed. Landing flaps neutral; propeller removed.

L-407

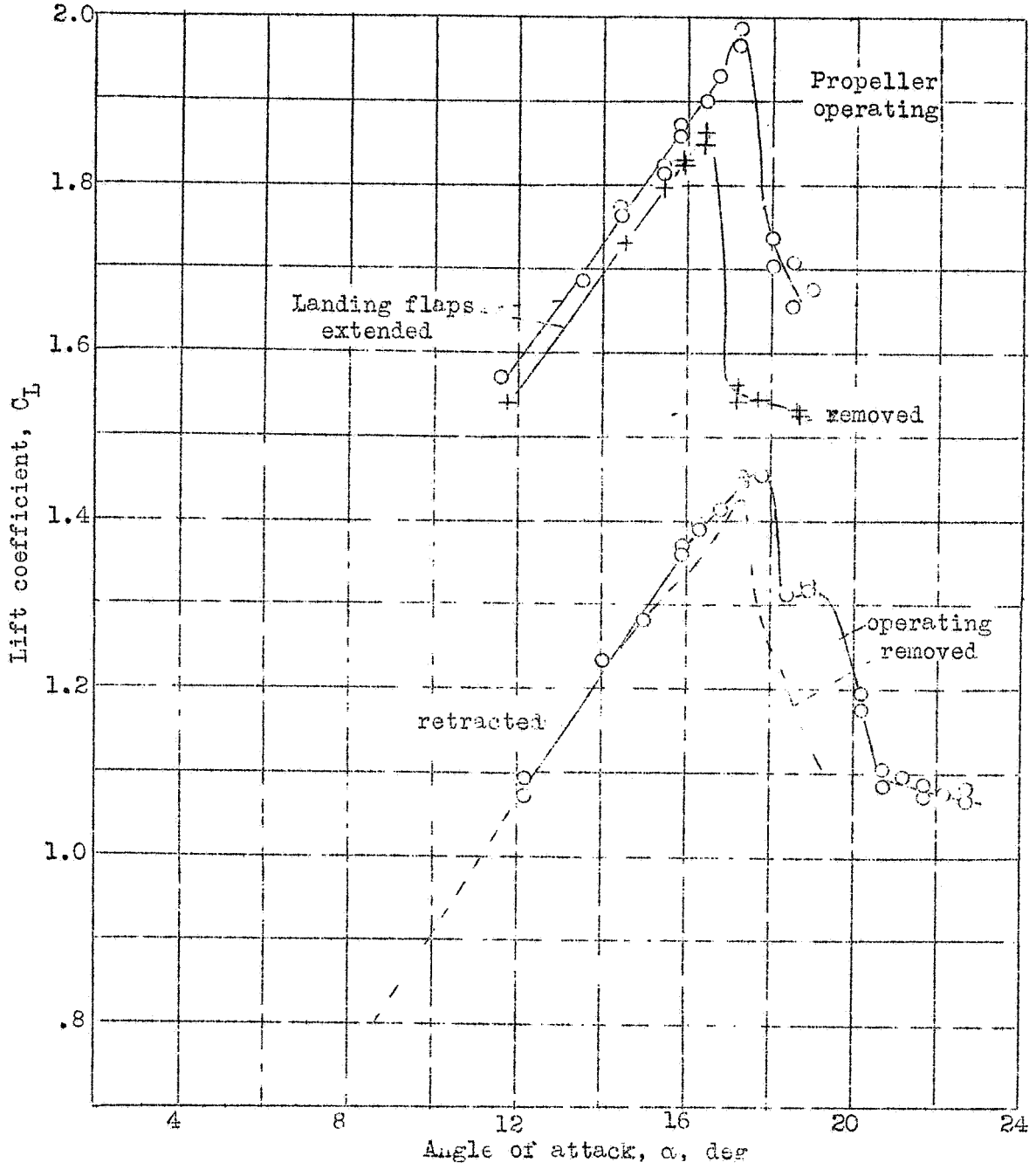

Figure 27.- Effect of propeller slipstream on the maximum lift coefficient of the complete model. Ducts installed in both wings; inlet 5; bottom outlet; outlet flaps closed; $\Delta p/q_p$, 5.8; $\beta = 38.5^\circ$; $T_c = 0.02$.